Molecular Ecology

WILEY

MOLECULAR ECOLOGY

ORIGINAL ARTICLE OPEN ACCESS

Genomic Signatures and Demographic History of the Widespread and Critically Endangered Yellow-Breasted Bunting

Guoling Chen | Simon Yung Wa Sin

School of Biological Sciences, The University of Hong Kong, Hong Kong, China

Correspondence: Simon Yung Wa Sin (sinyw@hku.hk)

Received: 9 July 2024 | **Revised:** 26 May 2025 | **Accepted:** 5 June 2025

Handling Editor: Christine Grossen

Funding: This work was supported by Research Grant Council, University Grants Committee (Hong Kong) (project number: 17124422) to S.Y.W.S.

Keywords: conservation genomics | genetic diversity | global climate change | inbreeding | mutation load | passerine

ABSTRACT

Population declines may have long-term genetic consequences, including genetic erosion and inbreeding depression, which could affect species' evolutionary potential and increase their risk of extinction. Small populations are more vulnerable to genetic threats than common species, but even species with large populations can also be at risk of extinction. The yellow-breasted bunting (*Emberiza aureola*) is a common and widespread songbird in the northern Palearctic regions, but its global population size has drastically declined by around 90% throughout the past 30 years, leading to an upgrade of its conservation status to critically endangered in the IUCN Red List. In this study, we identified three populations within this species using whole-genome resequencing data, but the genetic differentiation between populations was shallow. These populations underwent similar population fluctuations but differed in the extent of population decline, resulting in lower genetic diversity and more homozygous deleterious mutations in a population comprising individuals on islands. The ancient demographic history was mainly associated with the climate, while population declines over the past 100 generations are likely due to human activities. Our results suggest that the yellow-breasted bunting population before the recent collapse faced relatively low genetic threats and had high evolutionary potential. However, we should be vigilant about the genetic threats faced by this species, as our sampling time occurred at the onset of its recent global population collapse. This study provides valuable genetic information for the conservation of yellow-breasted bunting and also highlights the similar genetic threats faced by other large populations.

1 | Introduction

Many species are undergoing continuous population decline attributable to both climatic change and human activities (Cowie et al. 2022). Fluctuations in ancient climate have significantly impacted the population size of species (Nadachowska-Brzyska et al. 2015). Many species underwent range contractions and fragmentations in their distributions during glacial periods, while interglacial periods facilitated population expansion (Hewitt 2004; Holm and Svenning 2014; Nadachowska-Brzyska et al. 2015). In recent history, human activities have had an increasingly significant impact on biodiversity, emerging as one of the main causes of population decline and species extinction. Currently, more attention is being given to ecological and anthropogenic factors to prevent biodiversity loss and population decline. However, genetic information is often lacking

in conservation actions due to the challenges in obtaining the information and applying it directly to conservation management, despite their importance in species conservation (Kardos et al. 2016).

Population decline can result in various genetic consequences, including the loss of genetic diversity (Frankham et al. 2010; Gandra et al. 2021; Huynh et al. 2023). Genetic diversity is pivotal in a species' ability to adapt to changing environments. The loss of genetic diversity in a species can have a significant impact on its long-term evolutionary potential (Kardos et al. 2021). Another possible consequence of population decline is inbreeding and subsequent inbreeding depression (Keller and Waller 2002; Sin et al. 2021). Population decline may increase inbreeding, leading to inbreeding depression due to the exposure of deleterious mutations in homozygous state (Hedrick and Garcia-Dorado 2016). A previous study suggests that strong deleterious mutations are the main determinants of inbreeding depression, which may increase the risk of extinction (Kyriazis et al. 2021). Additionally, the number of these mutations in a population often correlates with the effective population size (Bertorelle et al. 2022). Smaller populations that persist for a long time tend to have more homozygous deleterious mutations, possibly due to the increase in inbreeding and genetic drift and less effective purifying selection in a small population (Bertorelle et al. 2022). In contrast, larger populations generally harbour more heterozygous deleterious mutations (Kyriazis et al. 2021). Consequently, larger populations are more susceptible to inbreeding depression if they undergo a rapid population decline (Bertorelle et al. 2022; van Oosterhout et al. 2022). This is because numerous recessive deleterious mutations may become exposed within a short timeframe, while natural selection may not have sufficient time to eliminate these deleterious mutations (Bertorelle et al. 2022; van Oosterhout et al. 2022). Moreover, even though some deleterious mutations can be eliminated by purifying selection, others may become fixed and negatively impact the overall fitness of the population (Glemin 2003; Grossen et al. 2020). Therefore, assessing genetic diversity, inbreeding level, and genetic load can provide valuable insights into the current genetic health and future viability of threatened species.

Endangered species, particularly those with small populations, often exhibit low genetic diversity and high inbreeding, which renders them more vulnerable to the "extinction vortex" (Blomqvist et al. 2010; Fagan and Holmes 2006). As a result, small populations usually receive more attention in conservation efforts than common species with large populations. Currently, the majority of research in conservation genetics focuses on small populations, such as the vaquita, killer whales, and Isle Royale wolves (Kardos et al. 2023; Robinson et al. 2022, 2019). In contrast, we may overlook population declines in common species despite their important role in maintaining ecosystem balance (Inger et al. 2015). Previous studies indicate that common European birds, such as the house sparrow and common starling, experienced more significant population declines compared to less abundant species (De Laet and Summers-Smith 2007; Inger et al. 2015; Smith et al. 2012). Indeed, large populations can also be at risk of extinction when faced with dramatic population fluctuations, like the passenger pigeon. In the early and mid-1880s, the passenger pigeon population was estimated to be 3–5 billion (Schorger 1995). Shockingly, it took only five decades for this abundant bird to become extinct. Previous studies suggest that a combination of dramatic population fluctuations and human activities may have ultimately led to the extinction of this species (Hung et al. 2014). Additionally, another study emphasised that although larger populations like the passenger pigeon exhibited the ability to eliminate harmful mutations and had developed traits to adapt to its environment, it could still face the risk of extinction following a sudden environmental change (Murray et al. 2017).

The yellow-breasted bunting (*Emberiza aureola*), which was historically one of the most abundant songbirds of the northern Palearctic region, is now facing a rapid population collapse similar to that of passenger pigeons (Hung et al. 2014; Kamp et al. 2015). They breed from northern and central Europe to far eastern Russia and Japan; most populations migrate towards the east, cross Siberia and northeast China, stop in the Yangtze Valley in China, and winter in Southeast Asia (BirdLife International 2024). Two subspecies were recognised for this species based on the geographical distribution and morphology, though the morphological differences were not distinct (Copete and Sharpe 2020; Park et al. 2020). The nominate subspecies *E. a. aureola* breeds from western Russia, through Kazakhstan and Mongolia, to eastern Europe, while *E. a. ornata* breeds in Transbaikalia, Mongolia, north-eastern China, far-eastern Russia, and Japan (Copete and Sharpe 2020; Park et al. 2020). The population size of this species was estimated to be hundreds of millions in the 1980s, but its numbers have drastically declined by 84.3%–94.7% between 1980 and 2013 (Kamp et al. 2015). Additionally, some populations (e.g., in Finland) have disappeared from certain breeding areas since the 2000s (Copete and Sharpe 2020; Tamada et al. 2017, 2014). Consequently, its conservation status was upgraded from Least Concern in 2000 to Critically Endangered in 2017 (BirdLife International 2024). This alarming situation highlights the need for conservation management to protect this species. Overhunting during the migration, agricultural intensification, and habitat destruction are believed to be the primary causes of the decline in the yellow-breasted bunting population (BirdLife International 2024; Kamp et al. 2015). However, it remains uncertain whether genetic factors contribute to this decline. A previous study provided some genetic information on this species (Wang et al. 2022). However, due to the limitations of the small sample size ($n = 10$) and the collection of samples during migration, information regarding the population structure, conservation units, changes in distribution range, and demographic history of different populations remains lacking.

In this study, we used whole genome resequencing data to investigate the demographic history and genetic consequences of population declines in yellow-breasted buntings. To delineate conservation units, we first determined the population structure of this species and examined gene flow between populations. We then reconstructed the ancient and recent demographic history of different populations and investigated the potential effect of paleoclimate on suitable breeding and wintering habitats of this species. Lastly, we investigated genetic diversity, inbreeding, and mutation load to assess the genetic health and evolutionary

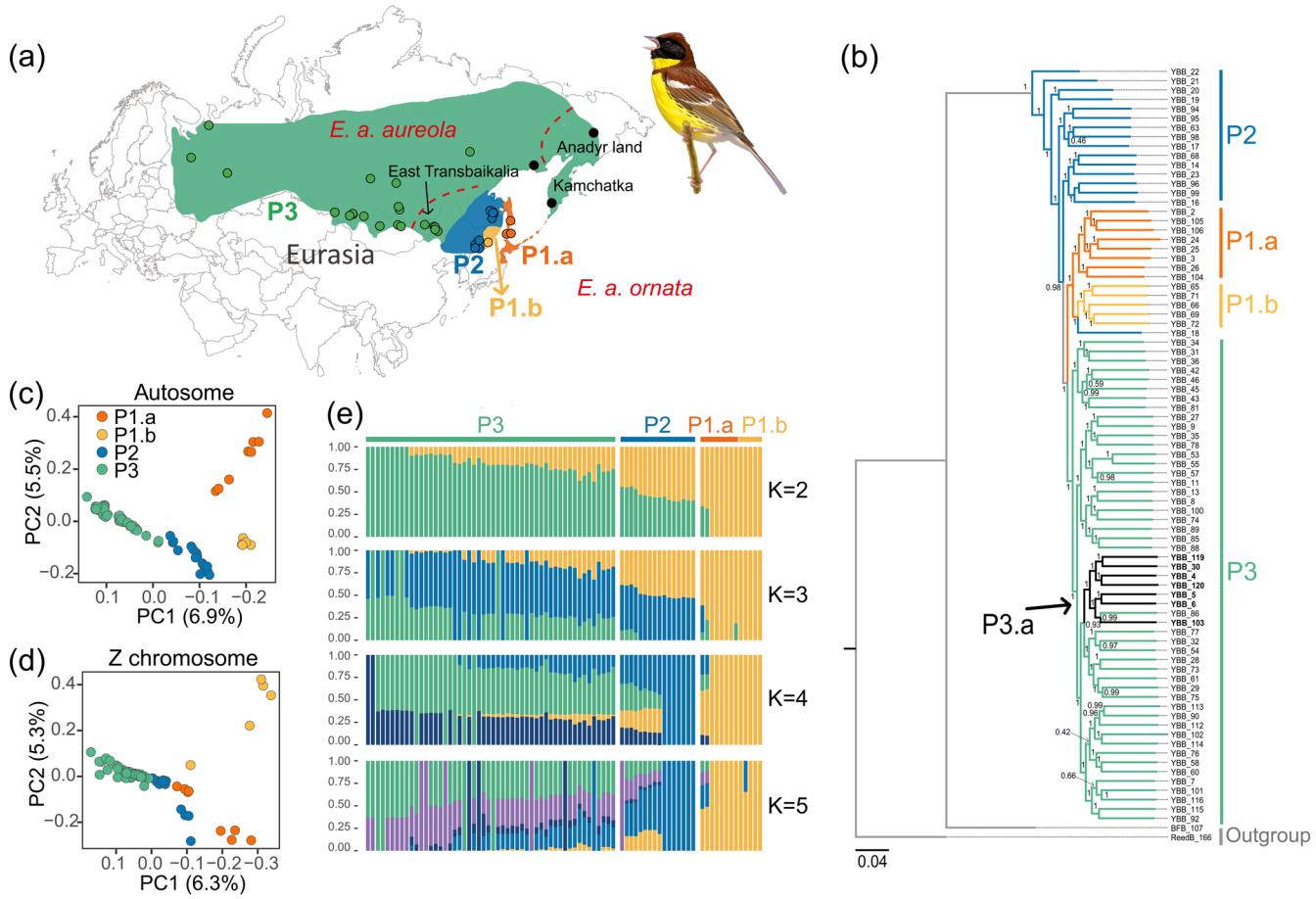

FIGURE 1 | The sampling sites and population structure of yellow-breasted buntings. (a) The map shows the breeding area and sampling sites of yellow-breasted bunting. Different colours indicate different populations in this study. Points indicate sampling locations. The red dashed lines indicate the boundaries of the proposed subspecies distribution (Copete and Sharpe 2020). The black dots indicate the locations where genetic population delimitation and subspecies disagree. (b) The maximum likelihood tree was inferred using FastTree based on the autosomal SNPs. Principal components analysis (PCA) for all the yellow-breasted bunting individuals based on (c) autosomal SNPs and (d) Z chromosomal SNPs. (e) Population structure inferred using Admixture with K ranging from 1 to 5. Each bar indicates one individual, and the y-axis indicates the probability of this individual being assigned to one or more clusters. Illustrations reproduced with permission of Lynx Edicions.

potential of the yellow-breasted bunting. Our study yields valuable insights into the mechanisms that contribute to endangerment in large populations and provides knowledge that can be used to develop effective conservation strategies for this critically endangered songbird.

2 | Materials and Methods

2.1 | Sample Collection

We acquired tissue samples from three bunting species, which included 120 yellow-breasted bunting (*Emberiza aureola*; only 81 samples were kept for the final analysis after filtering) and two outgroups (one black-faced bunting *E. spodocephala* and one reed bunting *E. schoeniclus*) from museum collections (Table S1). The samples were collected during the breeding season from 1992 to 2004, and the sampling sites of yellow-breasted bunting covered most of their breeding areas (Figure 1a). The tissue samples were stored in absolute ethanol at −80°C until DNA extraction.

2.2 | Genome Assembly and Annotation

One individual of yellow-breasted bunting was used for genome assembly (YBB_1; Table S1). High-quality genomic DNA was extracted from the tissue sample using the MagAttract HMW DNA Kit (Qiagen, Germany). The DNA quality was assessed using pulse-field gel electrophoresis, and a DNA library for whole genome sequencing was prepared using Chromium (10 × genomics). The library was sequenced on Illumina NovaSeq (PE 150 bp reads) by Novogene (Hong Kong).

We first processed the raw data by removing the low-quality data, adapters, and duplicated reads using FASTX-Toolkit v.0.0.14 (Hannon 2010) and FastUniq v.1.1 (Xu et al. 2012). Then, we corrected short-read errors using Musket v.1.1 (Liu et al. 2013). To check the quality of both the raw and clean sequencing data, we used FastQC v.0.11.7 (Andrews 2010). Next, we assembled the reference genome using Supernova v.2.1.1 (Zheng et al. 2016) with clean reads and summarised the assembly results (Table S2). To evaluate the completeness of the reference genome, we ran BUSCO v.5.3.2 (Simao et al. 2015)

analysis using the Aves dataset (aves_odb10) with 4915 universal single-copy orthologs (Table S3). Finally, we mapped the scaffolds of the yellow-breasted bunting draft genome to the zebra finch (*Taeniopygia guttata*) chromosome-level genome (GCA_008822105.2) from NCBI using Satsuma v.2 (Grabherr et al. 2010) to construct the pseudochromosomes.

To annotate the reference genome, we first identified and annotated the sequences of interspersed repeat using RepeatModeler v.2.0.2 (Flynn et al. 2020) and RepeatMasker v4.0.5 (Table S4) (Smit et al. 2020). We then trained ab initio gene predictors with the expressed sequence tags (ESTs) using SNAP in MAKER v.2.31.9 (Holt and Yandell 2011). The ESTs were obtained from the NCBI database, comprising the protein sequences of 15 avian species (Table S5). After that, the results of ab initio gene prediction, EST alignments, and protein alignments were combined to generate gene predictions in MAKER v.2.31.9. Furthermore, homology-based gene prediction was performed based on the nine avian species in GeMoMa v.1.7.1 (Keilwagen et al. 2019). Finally, the annotation results from MAKER v.2.31.9 and GeMoMa v.1.7.1 for the yellow-breasted bunting genome were combined using GeMoMa v.1.7.1 and then evaluated using BUSCO v.5.3.2 analysis (Table S6).

2.3 | DNA Extraction and Whole-Genome Resequencing

We extracted the genomic DNA of bunting tissues using the E.Z.N.A. Tissue DNA Kit (Omega Bio-tek, USA) following the manufacturer's protocol. The DNA quantity and quality were assessed using the Qubit dsDNA High Sensitivity Assay Kit on the Qubit 4 fluorometer (Thermo Scientific, USA) and agarose gel electrophoresis, respectively. Only high-quality DNA samples ($n = 94$; Table S1) were used for whole-genome resequencing. DNA libraries of 350 bp insert size were prepared, and sequencing was performed on Illumina NovaSeq (PE 150 bp reads) by Novogene (Hong Kong) to achieve 30 Gb data per sample.

2.4 | SNP Calling and Filtering

The raw data obtained from the whole-genome resequencing was filtered using Fastp v.0.23.2 (Chen et al. 2018), and the data quality was evaluated using FastQC v.0.11.7. The clean data was then aligned to the reference genome using Burrows-Wheeler Aligner (BWA v.0.5.17) (Li and Durbin 2009) with the default settings. Subsequently, we called the single nucleotide polymorphisms (SNPs) following the GATK v.4.1.4.0 (McKenna et al. 2010) Best Practices Workflows with Samtools v.1.19 (Li et al. 2009) and Picard v.2.26.6 (Broad Institute 2019).

To obtain a high-quality and credible SNP dataset, we first performed hard filtering (SOR > 3, FS > 60, MQRankSum <−12.5, ReadPosRankSum <−8, ReadPosRankSum > 8, MQ < 40, QD < 1) for SNPs using GATK v.4.1.4.0. We then performed soft filtering using VCFtools v.0.1.17 (Danecek et al. 2011) following these criteria: —minQ 30, —minDP 5, —maxDP 70, —max-missing 0.95, —max-alleles 2. We excluded the SNPs located on the 4–10 Mb section of chromosome 11 from all the analyses due to the higher number of missing SNPs in this region. After obtaining the results from Satsuma v.2, we extracted the SNPs of the autosomes and the Z chromosome. If additional filters, such as linkage disequilibrium (LD) pruning, were applied for a specific analysis, we would specify them in the relevant sections.

We used KING v.2.2.5 (Manichaikul et al. 2010) to calculate kinship coefficients for all pairs of individuals and excluded five individuals with 2nd-degree relationships (i.e., a kinship coefficient > 0.0884) from our dataset to avoid potential bias from closely related individuals. Additionally, we assessed the mean depth per site and missing rate for each individual and excluded eight individuals due to high missing rates. The remaining dataset consisted of 81 yellow-breasted buntings, one black-faced bunting, and one reed bunting that served as the outgroups for subsequent analyses.

2.5 | Population Structure and Phylogenetic Analysis

To avoid clustering bias caused by linkage disequilibrium (LD), we conducted LD pruning using PLINK v.1.9 (Purcell et al. 2007). For population structure and phylogenetic analysis, we also filtered out SNPs with minor allele frequency (MAF < 0.05). We then estimated population structure using autosomal SNPs, Z chromosomal SNPs, and the mitochondrial genomes. The mitochondrial genomes were assembled using MIRA v.4.0 (Chevreux et al. 2004) and MITOBIM.PL v.1.6 (Hahn et al. 2013). A yellow-breasted bunting mitochondrial genome (Pan et al. 2015) available on NCBI (accession no. NC022150.1) was used as the reference for the assembly of mitochondrial genomes.

We conducted three analyses to determine the population structure of yellow-breasted buntings. First, we performed principal component analysis (PCA) using PLINK v.1.9 based on autosomal and Z chromosomal SNPs. We also employed the R package adegenet v.2.1.10 (Jombart 2008; Jombart and Ahmed 2011), which can extract SNPs from the alignment, to perform PCA on mitochondrial data. Second, we reconstructed the maximum likelihood (ML) tree based on autosomal SNPs using FastTree v.2.1.11 (Price et al. 2010) with the General Time Reversible (GTR) model. Then, we reconstructed the ML tree using IQ-TREE v.2.1.3 (Minh et al. 2020) for the Z chromosomal SNPs and mitochondrial data. The best-fit substitution model for DNA sequences was determined by ModelFinder in IQ-TREE v.2.1.3. We used reed bunting as the outgroup and performed 1000 bootstraps for each analysis with UFBoot to estimate branch support. Finally, we estimated individual admixture proportions based on autosomal SNPs using ADMIXTURE v.1.3.0 (Alexander et al. 2009). We tested genetic clusters parameter K ranging from 1 to 6 and conducted each analysis with 200 bootstraps. The best K was determined based on the value of cross-validation error.

To reconstruct the potential spatial diffusion pathways for this species, we conducted a phylogeographical analysis as described in Edwards et al. (2011), using BEAST v.2.6.0 (Bouckaert et al. 2014). This method is based on the Bayesian stochastic search variable selection (BSSVS) model (Lemey et al. 2009), which helps to reconstruct the spatial dispersal patterns of

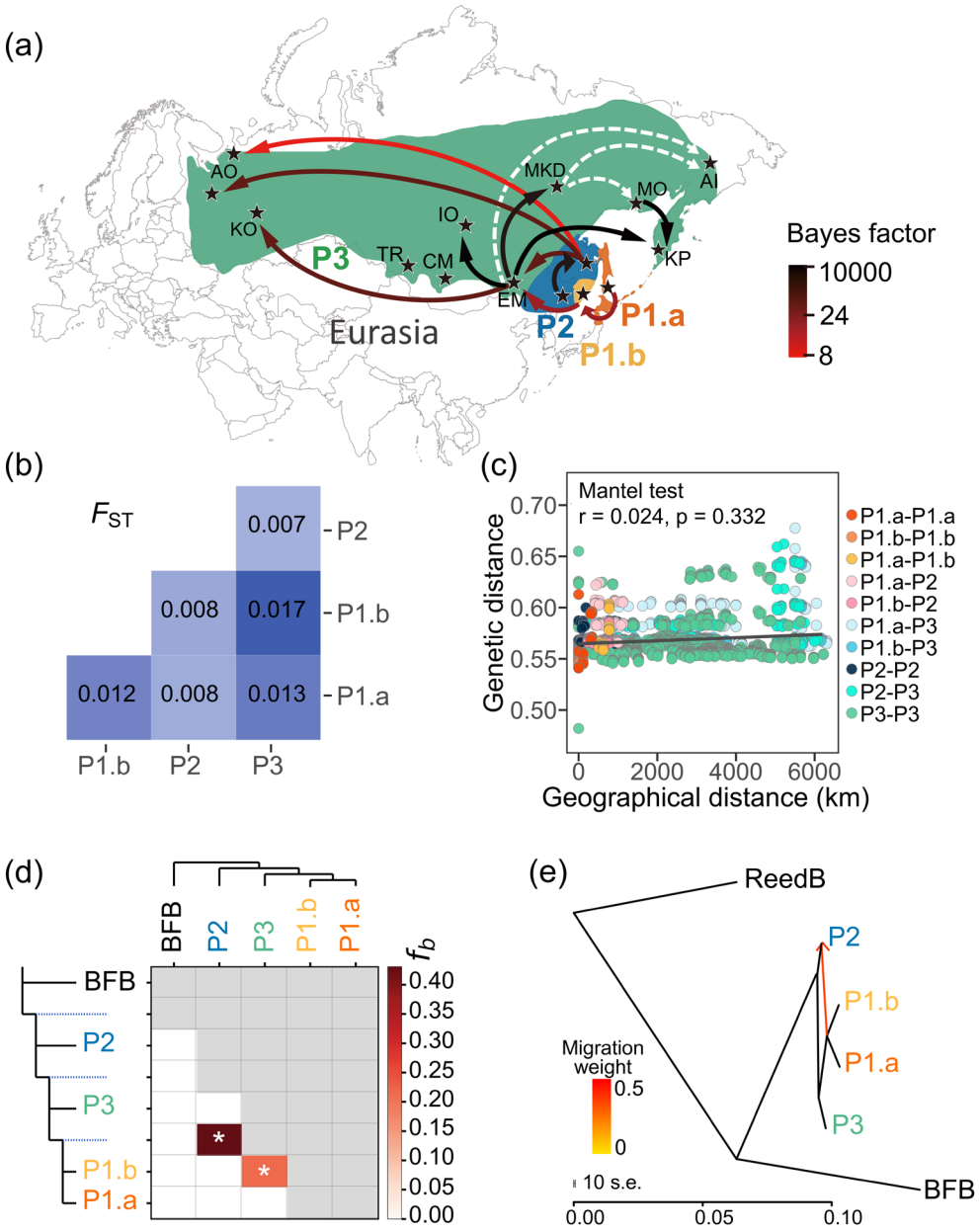

FIGURE 2 | The estimated spatial diffusion pathways, the genetic differentiation, and gene flow between different populations of yellow-breasted bunting. (a) The arrows indicate the reconstructed spatial diffusion pathways of yellow-breasted buntings between different locations. The significant pathways (Bayes factor > 8) are coloured from red to black, with darker arrows indicating higher significance. The three pathways highlighted in white are not significant, with a Bayes factor of 2–4. For the phylogeographic analyses, we assigned all individuals to 15 locations, which included two locations in P1 and P2, along with 11 locations in P3. AI, Anadyr land; AO, Arkhangelsk Oblast; CM, Central Mongolia; EM, East Mongolia; IO, Irkutsk Oblast; KP, Kamchatka Peninsula; KO, Kirov Oblast; MO, Magadan Oblast; MKD, Megino-Kangalassky District; TR, Republic of Tuva. (b) The matrix of genetic differentiation, F_{ST}, between different groups. The colour indicates the degree of genetic differentiation. (c) The correlation between the genetic distance and the geographic distance. The colour represents paired individuals from their corresponding populations. (d) The estimated gene flow using branch-specific statistic method (f_b) with Dsuite. The value in the matrix (f_b) indicates the excess allele sharing between populations. The asterisks (*) indicate significant f_b value ($p < 0.01$). (e) The estimated number and direction of migration events using Treemix. The colour of the arrows is based on the migration weight.

species by sampling time-scaled phylogenies. The Bayes factor test (Suchard et al. 2001) was used to assess the significance of the dispersal pathways, with a Bayes factor greater than eight typically considered significant. For the phylogeographic analyses, we categorised all individuals into 15 locations, which included two sites in P1 (P1.a and P1.b), two sites in P2, and 11 locations in P3, based on their sampling coordinates (Figure 2a).

We conducted 45,000,000 interactions of Markov Chain Monte Carlo (MCMC) simulations using 1,000,000 autosomal SNPs, with the initial 10% of interactions being designated as burn-in. To assess the robustness of our phylogeographic analyses, we performed a separate independent MCMC simulation that involved 40,000,000 interactions, which yielded results consistent with the first run.

To quantify the differentiation between populations, we estimated the genetic differentiation (F_{ST}) between the populations using VCFtools v.0.1.17 (Danecek et al. 2011). The pairwise F_{ST} was calculated using 20 kb non-overlapping sliding windows, and any windows with less than 50 SNPs were excluded from the analysis. Isolation by distance is a common model that illustrates the correlation between genetic divergence and dispersal among various geographic regions (Lam et al. 2023). To investigate whether the distribution of the yellow-breasted bunting population aligns with the pattern of isolation by distance (IBD), we conducted a correlation analysis between their geographic distance and genetic distance of all individuals, as well as those from P3 only. We calculated the genetic distance (D*ij*) between each pair of samples using RapidNJ v.2.3.2 (Simonsen et al. 2008), while the R package geosphere was used to calculate the geographic distance (Hijmans et al. 2017). To test the statistical significance in isolation by distance analysis, we carried out the Mantel test using the R package vegan v.2.6.8 (Dixon 2003). In addition, we performed isolation by distance analysis for each pair of populations. The geographical coordinates of the central point of each population were used to calculate the geographic distance between them. The correlation between the geographic distance and pairwise F_{ST} between populations was investigated.

To assess the potential bias introduced by different sampling years, we conducted a PCA of P1.a based on two different years: 1993 and 2003. Additionally, we performed a joint PCA of P1, which included P1.a from both 1993 and 2003 and P1.b.

2.6 | Estimation of Gene Flow

Three methods were used to estimate gene flow between different populations of yellow-breasted bunting. We calculated the Patterson's *D* statistic (also called ABBA-BABA statistics) for each trio of yellow-breasted bunting populations using the script developed by Simon Martin (https://github.com/simonhmartin/genomics_general). The setting of each trio is described in Table S7. The significance test, the block jackknife procedure, was applied to the mean genome-wide *D* values, with |Z| score > 3 indicating the *D* values deviate significantly from zero (Patterson et al. 2012). The significant deviation of *D* values suggests the presence of gene flow between populations A and C or populations B and C (Table S7). The second method involved estimating the *f-branch* (f_b) metric using autosomal SNPs with Dsuite v.0.5 (Malinsky et al. 2021). This approach extends from Patterson's *D* statistic, further distinguishes corrected *f*4-ratio results, and assigns gene flow evidence to specific branches on a phylogeny. The phylogeny used in this analysis was obtained from the ML tree of autosomal SNPs, where reed bunting and black-faced bunting were the outgroups. Individuals with uncertain phylogenetic relationships or hybrids of different populations were excluded from this analysis (Table S1). The significance of each f_b ratio was evaluated using the Z-scores and its associated *p*-values. The third method involved estimating the number and direction of past migration events using Treemix v.1.13 (Pickrell and Pritchard 2012) based on autosomal SNPs. To determine the appropriate number of migration edges (m) on the population tree, we inferred the optimal value of m using OptM v.0.1.8 (Fitak 2021). We ran 100 bootstrap replicates for each edge (from 1 to 10) with 1000 SNP blocks to account for the LD and find the best m. Finally, we used the matrix of residuals to establish metrics for evaluating the model's goodness of fit to the data.

2.7 | Inference of Demographic History

We used three methods to reconstruct the demographic history from ancient to recent times. We first inferred the changes in past effective population size from individual whole-genome sequences using pairwise sequentially Markovian coalescent (PSMC v.0.6.5) (Li and Durbin 2011). To avoid bias from low coverage and high missing data, we calculated each individual's sequencing coverage and missing rate. All 81 individuals had high-quality data and were used for PSMC analysis. These individuals had an average sequencing depth of 24.6×, with the lowest sequencing depth being 16.3×. The average missing rate was 0.46%, and only one individual had a missing rate greater than 10% (i.e., 13.2%). We mapped the clean reads of each individual to the reference genome using BWA and then called the SNPs using SAMtools v.1.19. The analysis excluded sex-linked SNPs. The PSMC was carried out with the default setting (-N25-t15-r5-p "4 + 25*2 + 4 + 6"), and the mutation rate was set to 6.9×10^{-9} per site per generation (2.3×10^{-9} per site per year) (Smeds et al. 2016). The mutation rate came from the collared flycatcher (*Ficedula albicollis*), as this data was not available for the yellow-breasted bunting. Based on previous studies, we set the generation time to 3 years (BirdLife International 2024).

We also inferred recent demographic history for each yellow-breasted bunting population using SMC++ v.1.15.2 (Terhorst et al. 2017). SMC++ uses a new spline regularisation method that combines site frequency spectrum (SFS) and LD information in coalescent HMMs to improve estimation accuracy (Terhorst et al. 2017). To avoid bias caused by selection and other factors, we excluded SNPs in the sex chromosome and coding regions. We performed SMC++ analysis with the following parameters: –polarisation-error 0.5, –spline piecewise, –regularisation-penalty 6.0, –knots 20. The mutation rate and generation time were the same as those used in PSMC. Additionally, we estimated the split time between different populations using SMC++. It is important to note that this method estimates the divergence time between populations, assuming no gene flow has occurred between them after the split (Terhorst et al. 2017). Based on our findings, we identified gene flow between the populations. Therefore, the split time inferred using this method might be slightly biased due to the effects of gene flow.

We estimated the effective population size of the past 700 generations using GONE (Santiago et al. 2020). This analysis was based on the observed spectrum of linkage disequilibrium (LD) of pairs of loci. We excluded the SNPs in the sex chromosome and coding regions. Due to the limitation of the software on the number of SNPs on each chromosome, we used scaffold-level data instead of pseudochromosome-level data for this analysis. Specifically, we used 191 scaffolds that were longer than 1 Mb

(73% of the total length of the autosomes), and the number of SNPs analysed in each scaffold was 50,000. We repeated the analysis 200 times for each population. We used the recombination rate (1.5 cM/Mb) of the zebra finch (*Taeniopygia guttata*) (Backstrom et al. 2010) in this analysis.

2.8 | Ecological Niche Modelling

To predict changes in species niches and distribution in past and future generations, we conducted ecological niche modelling (ENMs) analysis using Maxent v.3.4.4 (Phillips et al. 2006). This method applies a machine-learning technique called maximum entropy modelling to predict the most suitable conditions for a species based on environmental data and occurrence records. We obtained occurrence records from GBIF (https://www.gbif.org/species/2491518) and eBird (https://ebird.org/species/yebbun). We filtered the records based on the following criteria: for the prediction of the breeding habitat, we only used records from the breeding season (June to August) and within the breeding area; for the prediction of the wintering area, we used records from the wintering season (November to February) and within the wintering area. Then, we performed spatial thinning (keeping only one record within a range of 1 km^2). Then, we downloaded 19 bioclimatic variables from WorldClim (www.worldclim.org), but we excluded 10 bioclimatic variables from the analysis based on correlation analysis and permutation importance analysis (Table S8). Finally, we predicted the suitable breeding and wintering ranges of yellow-breasted bunting at the Last Interglacial (LIG), Last Glacial Maximum (LGM), Mid-Holocene (MH), the current day, and the year 2070. For the ENMs analysis of the year 2070, we ran the analysis under two Representative Concentration Pathways (RCP8.5 and RCP2.6) (van Vuuren et al. 2011), which represent the highest and lowest of the four greenhouse gas concentration pathways.

2.9 | Genetic Diversity and Inbreeding Analyses

To better understand the long-term evolutionary potential of yellow-breasted bunting, we estimated the genome-wide genetic diversity. We calculated the nucleotide diversity (π) based on 20 kb non-overlapping sliding windows using VCFtools v.0.1.17. Additionally, we estimated the genome-wide heterozygosity for each individual by dividing the total number of heterozygous sites by the effective length of the genome. In this section and the subsequent analysis, we employed different methods for significance testing based on the characteristics of the datasets. For datasets with a larger sample size ($n > 30$) that followed a normal distribution, we used the *t*-test. For datasets with a smaller sample size ($n < 30$) or those that did not conform to a normal distribution, we used the Wilcoxon test.

We estimated the inbreeding level by identifying the Runs of Homozygosity (ROH) using two methods, BCFtools v.1.14 (a hidden Markov model approach) and PLINK v.1.9 (a scanning window approach). The allele frequency obtained from all yellow-breasted bunting individuals, along with a constant recombination rate of 1.5 cM/Mb (Backstrom et al. 2010), was used in the BCFtools analysis. The analysis in PLINK was performed with the following settings: –mendel, –genome, –homozyg, –homozyg-group, –homozyg-window-snp 50, –homozyg-snp 50, –homozyg-window-missing 3, –homozyg-kb 100, –homozyg-density 50, –homozyg-window-het 3. We categorised the ROH into two types based on their length: short-ROH (0.1 Mb < ROH < 1 Mb) and long-ROH (ROH >= 1 Mb) (Ceballos et al. 2018). We defined the genome-wide inbreeding coefficient, F_{ROH}, as the total length of ROH divided by the effective length of the genome. Additionally, we estimated the distribution of ROH by calculating the S_{ROH} (total length of ROH) and N_{ROH} (total number of ROH). The estimated coalescent time (g) was calculated based on the length of ROH (L, Mb) following the formula $g = 100/2rL$ (E. A. Thompson 2013), with r (recombination rate) being 1.5 cM/Mb. Hence, the estimated time for short-ROHs was around 33–330 generations ago, while long-ROHs arose from the last 33 generations.

To evaluate the potential bias caused by different sampling timeframes, we categorised the samples into four time periods (1992 to 1994, 1997 to 1998, 2000 to 2001, and 2002 to 2004) and calculated genome-wide heterozygosity and F_{ROH} for samples from these four periods for each population.

2.10 | The Accumulation of Deleterious Mutations

To assess the genetic load in different populations of yellow-breasted bunting, we counted the number of deleterious mutations present in the genome. We first defined the derived alleles using the reed bunting as an outgroup. If an allele is present in the yellow-breasted bunting population and has a zero frequency in the outgroup, it is classified as a derived allele. Then, we used snpEff v.4.3 (Cingolani et al. 2012) to annotate the functional effect of derived alleles, categorising them as loss-of-function (LoF) variants, nonsynonymous variants, and synonymous variants. LoF variants are considered the most harmful mutations and contain variations with splice donor, splice acceptor, start lost, stop lost, stop gained, and stop retained mutations. Nonsynonymous mutations were further classified into two groups based on Grantham's score (Grantham 1974): deleterious (Grantham's score > 150) and tolerated (Grantham's score = < 150) nonsynonymous mutations. The synonymous variants were considered neutral.

We calculated the total number of four types of mutations—LoF, deleterious nonsynonymous, tolerated nonsynonymous, and synonymous mutations—for each individual. We also calculated the number of homozygotes and heterozygotes for these four types of mutations. The number of these four types of mutations was normalised by the total number of derived mutations of each individual. Additionally, we used the ratio of deleterious mutations to neutral mutations as the index of effectiveness of purifying selection (Robinson et al. 2022). We calculated the ratio of LoF, deleterious nonsynonymous, and tolerated nonsynonymous mutations for each population of yellow-breasted bunting. We also calculated the index of relative allele frequency (R_{xy}) for the three categories of deleterious mutations using a custom script. The R_{xy} values were calculated following the method of a previous study (Xue et al. 2015), and these R_{xy} values were normalised using intergenic variations. To estimate the standard deviation

of the R_{xy} values, we performed 100 rounds of data resampling using a block jackknife approach.

2.11 | Simulations

To evaluate the impact of recent demographic history on the accumulation of deleterious mutations, we performed forward simulations with the Wright-Fisher (WF) model using SLiM v.4.0.1 (Haller and Messer 2023). We simulated the demographic scenarios of each population before their split (around 30,000 years ago) based on the demographic history obtained from GONE and SMC++. To reduce computational time, we scaled down the effective population size of each population to 0.05-fold. According to standard procedure, the mutation and recombination rates should be rescaled by a factor of 20. However, due to limitations in computing resources, we were only able to rescale these rates by 10-fold. To mitigate potential bias from this rescaling factor, we conducted tests with various rescale factors. Our findings indicated that while the absolute number of deleterious mutations was affected by the rescale factor, there was minimal impact on the relative patterns observed among different populations. This suggested that using a 10-fold rescale factor would not compromise the interpretation of our results. We simulated a genome with 3500 genes for each individual, which is around 20% of the reference genome. Each gene has a length of 1500 bp. These genes were distributed across five chromosomes. The mutation rate was set to 6.9×10^{-9}, and the recombination rate within genes was set to 1.5×10^{-8}. We assumed no recombination between genes, while the recombination between chromosomes is free. The proportion of deleterious mutations was defined based on the distribution of fitness effect (DFE), which was calculated using polyDFE v.2.0 (Tataru and Bataillon 2019). This method employs maximum likelihood (ML) inference, enabling the simultaneous fitting of DFE parameters and nuisance parameters based on the unfolded site frequency spectrum (SFS) data. We evaluated two types of distribution models (Models A to C) with varying parameters following the polyDFE tutorial. The final DFE model was selected based on the Akaike Information Criterion (AIC) results. Nevertheless, accurately estimating a DFE remains a challenge for non-model species. To evaluate the impact of DFE, we conducted an additional independent simulation using the DFE of humans (Kim et al. 2017). We modified the "hmix" model based on the previous studies (Kyriazis et al. 2023, 2021) for the setting of dominance coefficients.

To conduct our simulations, we first ran a burn-in period of 10 times the effective population size. During this period, we sampled the data every 1000 generations. After the burn-in period, we sampled the data every two generations. For data collection, we obtained data from a sample of 100 individuals from the population. The data we collected during the simulation included four types of mutations: strongly deleterious ($s\leq-0.01$) and weakly deleterious ($-0.01<s\leq-0.00001$), and neutral alleles ($s=0.0$). We computed the realised load, which captures the total expressed load of all homozygous deleterious mutations. Furthermore, we assessed the fitness of individuals, which was calculated based on the selection coefficient and dominance coefficient of deleterious mutations in each individual. We conducted 50 replicates for each simulation.

3 | Results

3.1 | Genome Assembly and SNP Calling

We achieved 132 GB of data for genome assembly. The reference genome size was estimated as 1.13 Gb, with a scaffold N50 of 4.57 Mb and a contig N50 of 115 kb (Table S2). BUSCO analysis showed that the reference genome had 91.5% completeness (Table S3). We annotated 16,671 protein-coding genes for the reference genome (Table S6). We performed whole-genome resequencing on 94 yellow-breasted bunting individuals and two outgroups. After filtering, 81 yellow-breasted bunting individuals were used for the subsequent analyses (Figure 1a, Table S1). The average number of reads mapped to the reference genome was 199,977,156 (range from 146,808,532 to 234,193,358), the mean depth per individual was 24.6× (range from 16.3× to 28.8×), and the mean missing rate was 0.46% (range from 0.06% to 6.34%). Lastly, we identified 145,174,637 autosomal biallelic SNPs and 1,319,040 Z-linked SNPs after filtering for downstream analyses.

3.2 | Population Structure and Gene Flow

We used three methods to estimate the population structure and genetic divergence within this species. The ML tree based on autosomal SNPs formed three main populations: populations P1 and P3 were monophyletic clades, while P2 was paraphyletic to P1 and P3 (Figure 1b). P1 was further divided into two monophyletic subpopulations, P1.a and P1.b. A similar pattern was also observed in the ML tree based on Z-linked SNPs, although the clusters of P2 were unstable (Figure S1). The PCA results based on autosomal and Z chromosomal SNPs (Figure 1c,d) were consistent with the phylogenetic tree: three main clusters were formed, with P1 divided into two clusters on PC2 and P2 in the middle of P1 and P3. The result of Admixture mainly supports the populations of P1 and P3, while the population P2 appears to be a mixture of P1 and P3 (Figure 1e). K = 1 is the most supported number of clusters based on the result of CV error. However, the optimised K can be unreliable, especially when the population differentiation is shallow (Kalinowski 2011). Moreover, according to the ML tree results, P2 did not form a monophyletic clade with the other two populations. We therefore consider P2 to be a different population and hypothesise that it could be the parental population (see Section 4). Both F_{ST} and the mitochondrial genome results suggest that the genetic differentiation between these populations was very shallow. The average genome-wide F_{ST} between these populations is lower than 0.02, with the highest F_{ST} between P1 and P3, particularly P1.b and P3 ($F_{ST}=0.017$), and the lowest F_{ST} between P2 and P3 ($F_{ST}=0.007$) (Figure 2b). Moreover, no clear structure was found in the PCA and ML tree based on the mitochondrial genomes (Figure S2). This could be due to the shallow differentiation between different populations and the relatively small amount of genetic information provided by the mitochondrial data.

The populations of yellow-breasted buntings were associated with the geographical distribution (Figure 1a). P1 was located in the eastern regions, including the island population (P1.a: Sakhalin, Japan, and Kuril Islands) and coastal areas (P1.b: Primorskiy). P2 was located in the North-Eastern Asia,

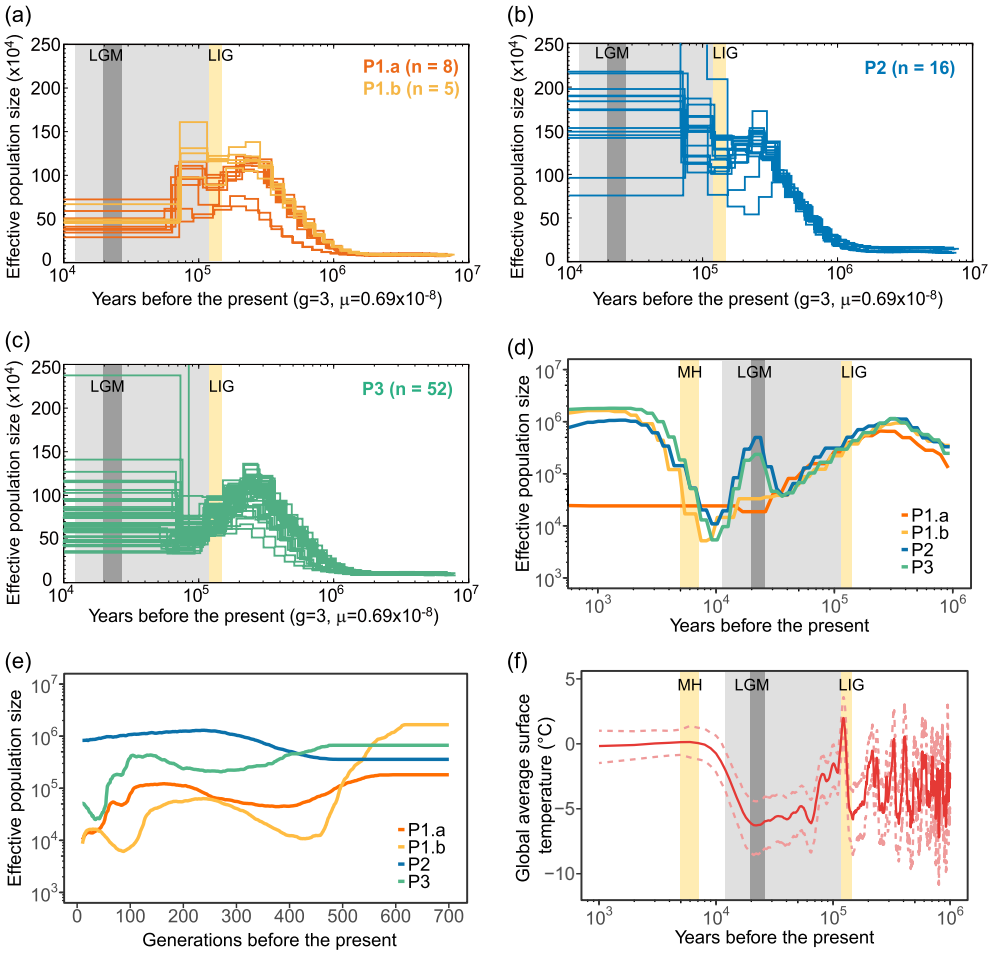

FIGURE 3 | Demographic histories of yellow-breasted buntings. (a) Demographic history of the population (a) P1.a and P1.b, (b) P2, and (c) P3 based on the individual autosomal SNPs using pairwise sequentially Markovian coalescent (PSMC). (d) The inference of effective population size using SMC++. (e) The estimation of effective population size in the past 700 generations using GONE. (f) The changes in global average surface temperature in the past millions of years. The yellow colour blocks indicate the Last Interglacial (LIG, 130,000 to 115,000 years before present (YBP)) and Mid-Holocene interglacial periods (7000 to 5000 YBP), respectively. The light grey colour block indicates the Last Glacial Period (LGP, 115,000 to 11,700 YBP), while the dark grey colour block indicates the Last Glacial Maximum (LGM, 26,000 to 20,000 YBP).

between P1 and P3. P3 occupied most of the distribution range from Finland, Mongolia, to Eastern Siberia. The results of the phylogeographic analysis suggest two potential dispersal pathways leading from P2 and P1.b to East Mongolia (P3) (Figure 2a). East Mongolia may serve as the primary source for the remaining groups of P3, particularly those in the western and northern breeding areas. Additionally, P2 may also be a potential source for the Arkhangelsk Oblast population. Although these populations were highly correlated with geographic distribution range, they did not show an "isolation by distance" relationship based on genetic distance between individuals (Figure 2c) nor the pairwise F_{ST} between populations (Figure S4a). Isolation by distance was also not observed within population P3 (Figure S4b).

Three methods were applied to investigate whether the weak differentiation among these populations was caused by gene flow. Patterson's *D* statistics revealed significant gene flow between populations P2 and P3, as well as gene flow between P2 and P1.a and gene flow between P3 and P1.a (Table S7). The result of the *f-branch* (f_b) metric identified two significant gene flows between these populations (Figure 2d). Most of the migration events occurred between P2 and P1 ($f_b = 43.04\%$), and the migration events between P3 and P1.b amounted to 21.55%. Treemix results indicate one migration edge (m) on the population tree, suggesting that gene flow happened between P2 and P1 (Figure 2e, Figure S3).

3.3 | Demographic History and Climate Change

The PSMC analysis based on individual genomes supported similar population size fluctuations of the three populations in ancient history (Figure 3a–c). All populations showed an effective population size expansion before the Last Interglacial (LIG), followed by different degrees of population decline. The population size of P1 continued to decline during the last glacial period (LGP), while the population size of P3 showed a similar decline but rebounded slightly during the LGP. In contrast, the population size of P2 did not show a significant decrease even after the LIG.

The relatively recent demographic history inferred using SMC++ suggested that these populations shared similar

demographic trajectories before the Last Glacial Maximum (LGM) but showed different responses to LGM (Figure 3d). This observation is supported by the divergence time estimated using SMC++, which indicates that the split between the three pairs of populations occurred around the beginning of LGM (Figure S5). After the populations split, the population size of P1.a had been stable but relatively low since the LGM, while the population size of P1.b showed an expansion during the mid-Holocene (MH) period after a long-term decline. On the other hand, the population size fluctuation of P2 and P3 was similar. Both populations rebounded before LGM and declined again since the LGM, and they increased in population size again after entering MH.

We further inferred the changes in the population size over the past 700 generations (~2100 years) using GONE. P1.a, P1.b, and P3 experienced similar population trajectories, all undergoing a bottleneck during the 300–500 generations and a population decline in the past 100 generations (Figure 3e). The effective population size of P1.a and P1.b was lower than that of P3. However, the population size of P2 remained high and stable over the past 700 generations. Therefore, P1.a and P1.b experienced a more severe recent population decline than the other two populations.

Fluctuations in effective population size of these populations appear to be highly related to climate change. The changes in global average surface temperature (Snyder 2016) were consistent with the fluctuation pattern of effective population size (Figure 3f). During most of the LGP, with lower temperatures, most populations experienced a population decline. In contrast, most populations except P1.a underwent a population expansion during the warmer MH period. Moreover, climate change also impacted the suitable breeding area (Figure 4). The ENM results indicated that the breeding range of the yellow-breasted bunting underwent a contraction during the LIG period compared to its existing distribution area and the N_e of the three populations also began to decline. The suitable breeding range reached a minimum during the LGM period, with an overall shift towards the south. The N_e of these populations is either at a minimum or experiencing a sharp decline. The breeding habitat showed an east–west discontinuity during the LIG and LGM periods. However, during the MH period, suitable habitats increased with the rise in temperature, with population expansion observed in these populations except for P1.a. Unlike the breeding range, the wintering area did not show obvious differences in the ancient period (Figure S6).

To investigate the impact of climate change on the yellow-breasted bunting in future generations, we further predicted the suitable breeding and wintering area of this species in year 2070. We conducted the ENM analysis based on different climate change scenarios, specifically, the Representative Concentration Pathways (RCP) 2.6 and 8.5. Both ENM results suggest that there will be a contraction in the suitable breeding area in the year 2070, especially in the middle regions (i.e., Mongolia and NE Asia) and the eastern regions (i.e., coast and islands) (Figure 4e,f). In contrast, there are no significant impacts on the wintering area in year 2070 (Figure S6e,f).

3.4 | Genetic Diversity and Inbreeding

Genetic diversity is a critical factor that reflects the long-term evolutionary potential of a species, which could be affected by demographic history and inbreeding. The mean nucleotide diversity of yellow-breasted bunting was 5.67×10^{-3}, and the average nucleotide diversity for each population was 5.44×10^{-3}, 5.78×10^{-3}, 6.00×10^{-3}, and 5.57×10^{-3} for P1.a, P1.b, P2, and P3 respectively. The overall genome-wide heterozygosity was 4.88×10^{-3}, and the average heterozygosity was 4.67×10^{-3}, 4.87×10^{-3}, 5.13×10^{-3}, and 4.84×10^{-3} for P1.a, P1.b, P2, and P3, respectively. Our results indicate that P1.a has a significantly lower nucleotide diversity and genome-wide heterozygosity than the other populations (Figure 5a,b). This might be due to the long-term population decline and the relatively low effective population size of this population. In contrast, P2, which experienced a large and stable population size, has higher nucleotide diversity and genome-wide heterozygosity than other populations.

The inbreeding levels varied among different populations of yellow-breasted buntings. P1.a and P1.b have a significantly higher F_{ROH} than P2 and P3, based on the ROH identified using BCFtools (Figure 5c). A similar pattern was observed in the results of ROH identified with PLINK, although only the difference between P1.b and P3 is significant (Figure S7a). This trend is also observed in short-ROH (0.1 Mb < ROH < 1 Mb), while the difference in long-ROH (ROH >= 1 Mb) was not significant (Figure S7b,c). The distribution of short-ROH shows that P1.a and P1.b have relatively more and longer ROH than the other two populations, indicating that P1.a and P1.b have smaller populations over the past 33 to 330 generations (Figure 5d). In contrast, there was no obvious difference in the distribution of long-ROH between these populations.

To evaluate the impact of sampling periods on genetic diversity and inbreeding, we calculated these characteristics across four distinct time periods. No temporary significant effect on genome-wide heterozygosity and F_{ROH} was shown across various time periods within each population (Figure S8a–d). Besides, the temporary sampling of P1.a did not affect the inferred population structure between P1.a and P1.b (Figure S8e,f).

3.5 | The Accumulation of Deleterious Mutations

P1.a has accumulated more homozygous deleterious mutations of three types compared to P2 and P3, while P1.b has accumulated more homozygous deleterious and tolerated nonsynonymous mutations than P2 and P3 (Figure 6a). However, the difference between the total number of deleterious mutations and heterozygous deleterious mutations was insignificant among these populations, except P2 has a higher number of tolerated deleterious mutations than the other populations (Figure S9). On the other hand, population P2 has the lowest number of homozygous LoF, deleterious nonsynonymous, and tolerated nonsynonymous mutations.

We evaluated the effectiveness of purifying selection using two methods, the ratio of deleterious mutations to neutral

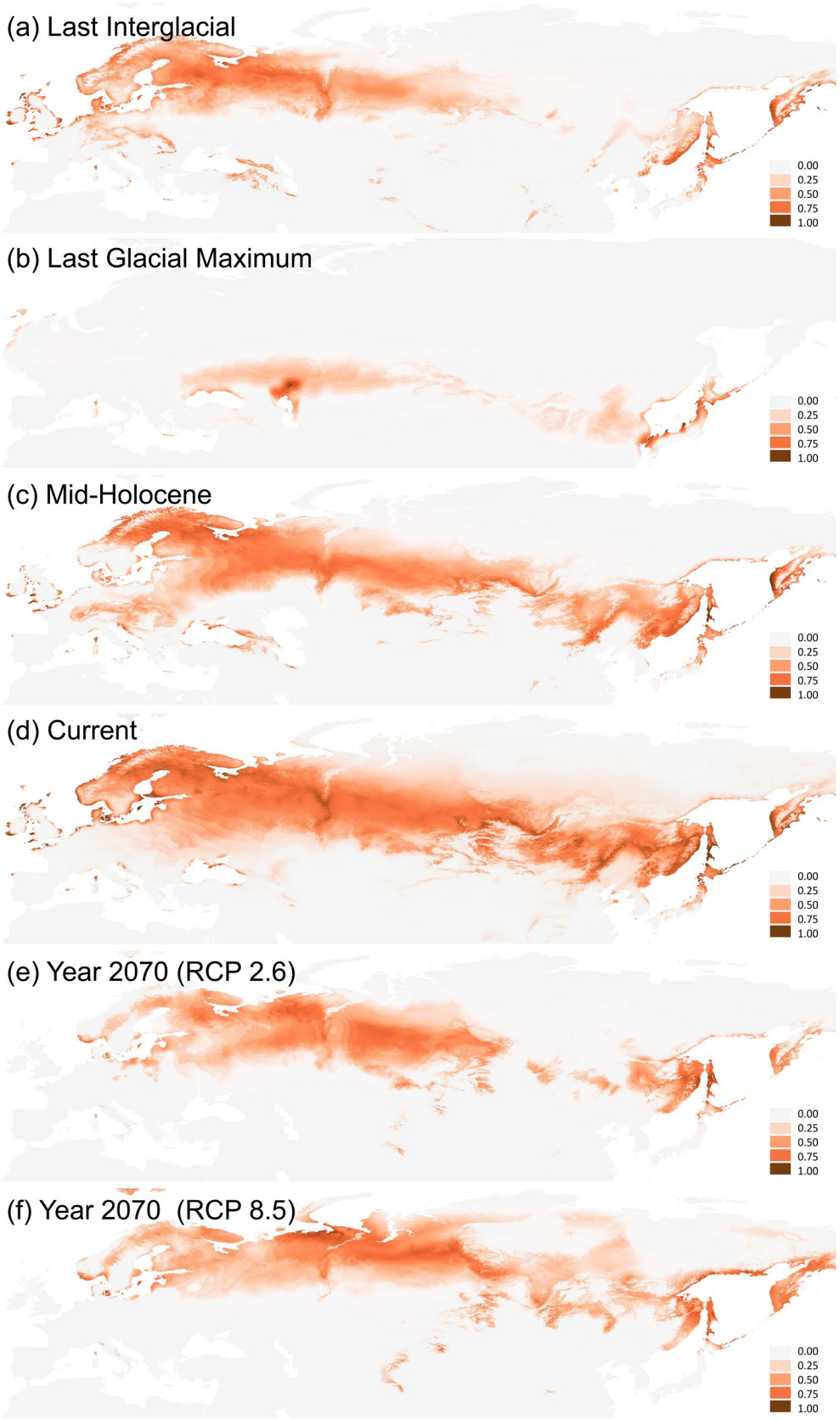

FIGURE 4 | The predicted suitable breeding range of yellow-breasted bunting. Reconstruction of ecological niche models for the breeding area of yellow-breasted buntings in the Last Interglacial (LIG), Last Glacial Maximum (LGM), Mid-Holocene (MH), current, and year 2070 with different Representative Concentration Pathways (RCP2.6 and RCP 8.5). The colour indicates the probability of suitable conditions in the models (i.e., darker colour indicates more suitable).

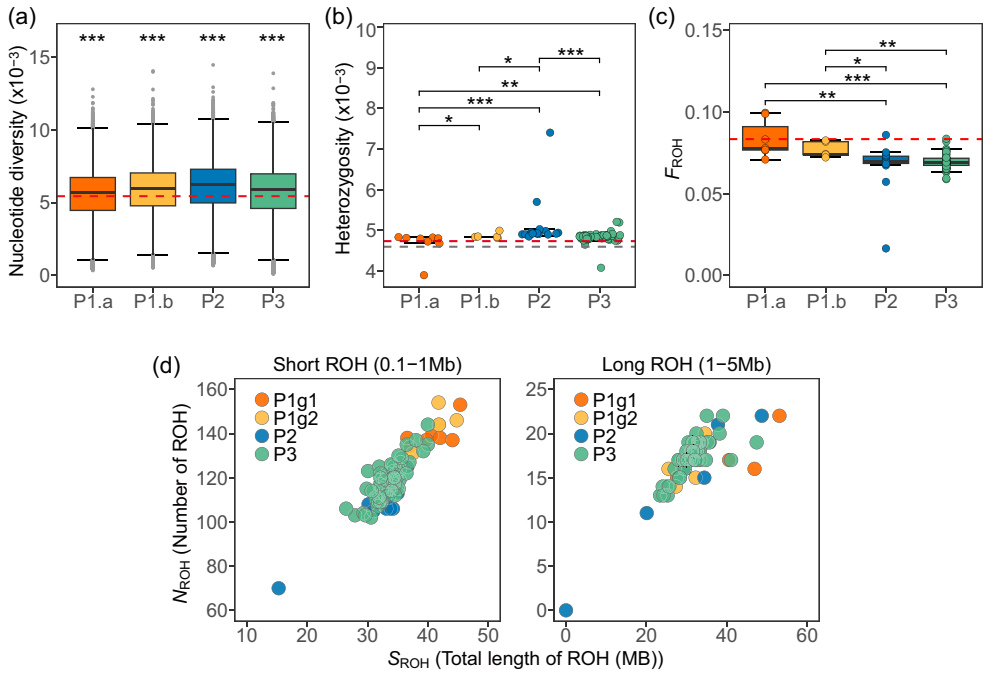

FIGURE 5 | The genome-wide genetic diversity and level of inbreeding of yellow-breasted buntings. The estimated (a) average nucleotide diversity and (b) genome-wide heterozygosity of different populations of yellow-breasted buntings. (c) The genome-wide inbreeding coefficient, F_{ROH}, of different populations. ROHs longer than 100 kb were included in this analysis. The red dotted lines in (a), (b), and (c) indicate the mean nucleotide diversity, mean genome-wide heterozygosity, and mean F_{ROH} of population P1.a. The grey dotted line in (b) indicates the mean genome-wide heterozygosity (i.e., 4.6×10^{-3}) of yellow-breasted buntings collected in 2019 based on Wang et al. (2022). (d) The distribution of the total number of ROHs and the total length of ROHs is shown for two categories of ROHs. Short-ROH (left): Ranges from 0.1 to 1 Mb; long-ROH (right): Longer than 1 Mb. The ROHs in (c) and (d) were identified from BCFtools. The '***' in (a) indicates that the differences between all population pairs are significant. In (b) and (c), significant differences between population pairs are indicated by asterisks (*). *$p<0.05$; **$p<0.01$; ***$p<0.001$.

mutations and the relative frequency of derived alleles (R_{xy}). The effectiveness of selection is associated with the effective population size, with larger populations generally experiencing stronger selection. Our results indicate that the differences in the ratio of deleterious mutations are insignificant among most populations, except that P2 has a significantly lower ratio of LoF, deleterious, and tolerated nonsynonymous mutations compared to the other populations (Figure 6b). The R_{xy} values indicate that LoF mutations were significantly higher in P1.a compared to other populations, while P2 accumulated more tolerated nonsynonymous mutations than the other populations (Figure 6c).

To investigate whether the accumulation of homozygous deleterious mutations in P1 is due to demographic changes, we simulated the demographic scenarios for these populations before their split. The simulation results indicate that P1.a and P1.b have accumulated more homozygous deleterious mutations (including strongly and weakly deleterious mutations) and a higher realised load than P2 and P3 under corresponding demographic scenarios (Figure 6d,e). In addition, population P2 has accumulated fewer homozygous deleterious mutations and a lower realised load than other populations. Hence, P1.a and P1.b were found to have lower fitness, and P2 demonstrated the highest fitness, which negatively correlates with the results of realised load (Figure 6f). To assess the impact of DFE, we also conducted simulations based on the DFE of humans. The simulations using both DFEs indicated a similar pattern among the populations; however, the difference in the number of homozygous deleterious mutations between P2 and P3 was more pronounced in the simulations that used the human DFE (Figure S10).

4 | Discussion

4.1 | Shallow Genetic Differentiation Among Yellow-Breasted Bunting Populations

We have identified three populations of the yellow-breasted bunting with shallow genetic differentiation between them. Our findings suggest that the genetic divergence among these populations is primarily associated with their geographic distribution, spanning from east to west. The genetic differentiation between these populations was notably low ($F_{ST}<0.02$), possibly due to gene flow between them. All three methods have uncovered gene flow between P2 and P1, and some methods have identified gene flow between P3 and P1.a or P1.b, as well as between P3 and P2. The inconsistency in the results of these methods could be due to the strength of gene flow and the limitations of the methods. Previous studies suggest the strength of gene flow, the direction of gene flow, the number of SNPs, the migration between the other populations in the test groups, and the effective population size can impact the accuracy of *D* statistics and *f*-branch statistics (Malinsky et al. 2021; Patterson et al. 2012; Peter 2016; Zheng and Janke 2018). These methods may not detect every gene flow event and are most robust when gene flow is particularly strong (Malinsky et al. 2021). Prior research indicates that the uneven gene flow between populations may be

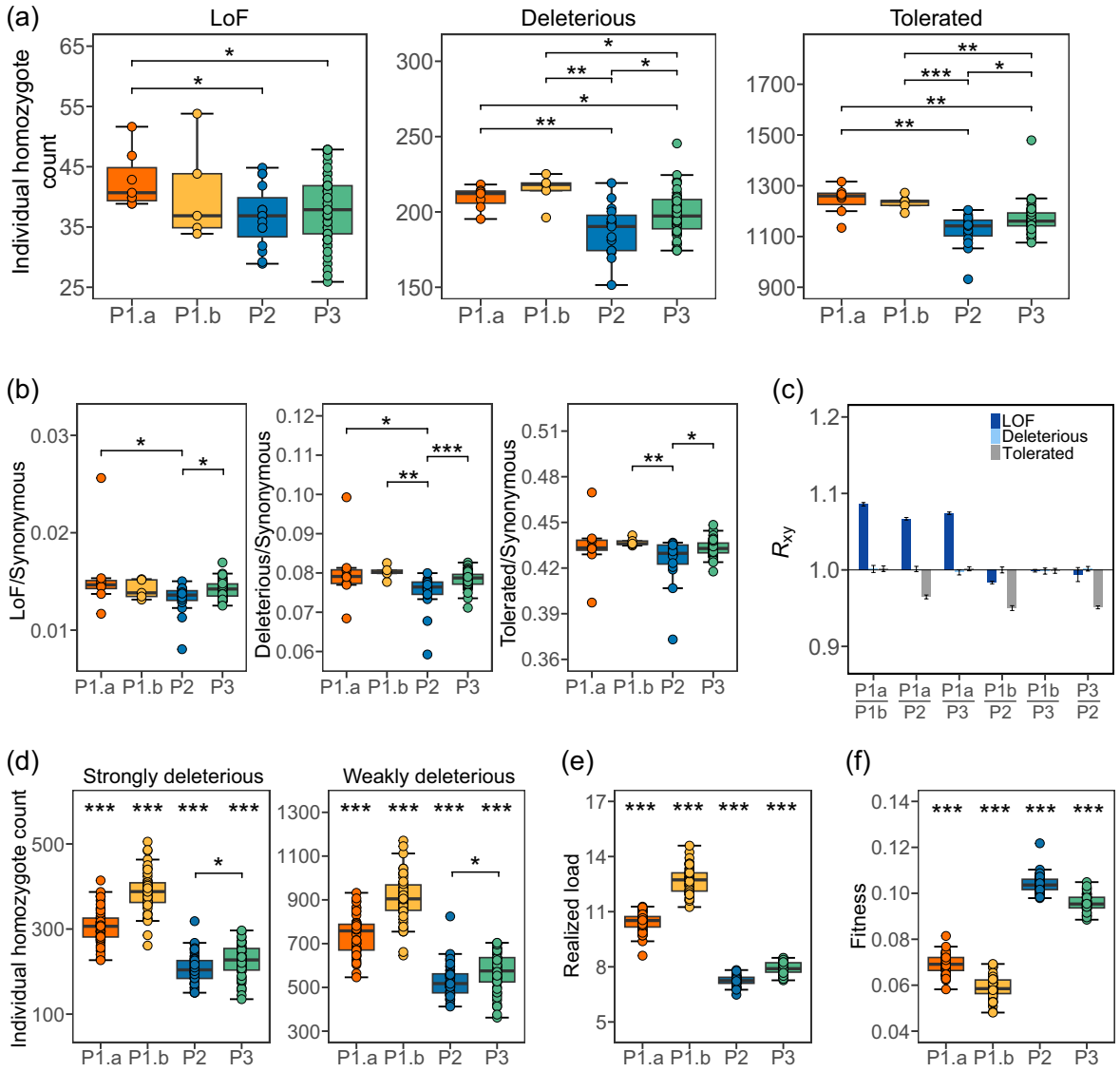

FIGURE 6 | The accumulation of deleterious mutations in the yellow-breasted bunting populations. (a) The number of homozygous loss-of-function (LoF), deleterious nonsynonymous, and tolerated nonsynonymous mutations per individual. (b) The ratio of LoF, deleterious nonsynonymous, and tolerated nonsynonymous mutations to synonymous mutations. (c) Relative frequency of derived mutations at LoF, deleterious, and tolerated sites between different populations. $R_{xy} > 1$ indicates excess relative frequency in the populations shown in the top panel, and $R_{xy} < 1$ indicates excess relative frequency in the populations displayed in the lower panel. (d) The number of homozygous strongly and weakly deleterious mutations, (e) the realised load per individual based on the simulations of the demographic history of the yellow-breasted bunting populations. (f) The fitness of individuals in different populations during simulations. We simulated the demographic scenarios of different yellow-breasted bunting populations since their split in the Last Glacial Maximum (LGM) period. In (a) and (b), the significant differences between population pairs are indicated by asterisks (*). The *** in (d–f) indicates a significant difference with $p < 0.001$ between all population pairs except the pair of P2 and P3. *$p < 0.05$; **$p < 0.01$. ***$p < 0.001$.

attributed to geographic distances within species (Wang 2013; Wang et al. 2013). However, the genetic distance of the yellow-breasted bunting does not follow the pattern of isolation by distance (IBD). This could be attributed to P3 occupying the majority of the distribution area, with minimal differentiation within P3, while the primary genetic divergence occurs between P1 and P3, leading to the absence of IBD.

Based on the population structure and geographic distribution of these populations, we have formulated two hypotheses that could explain the population structure of the yellow-breasted bunting. First, population P2, situated in the middle, may represent an admixed population of P1 and P3. Second, population P2 may serve as the primary population of yellow-breasted buntings, with P1 and P3 expanding to the east and west from P2, respectively. This hypothesis is predominantly based on the autosomal phylogenetic tree, which situates P2 at the tree's root. The results of phylogeographic history strongly indicate that P2 was one of the potential sources for P3 (both East Mongolia and Arkhangelsk Oblast). We did not detect any possible dispersal pathways leading to P2. Furthermore, P2 had a larger and more stable effective population compared to the other two populations, suggesting its role as the primary population. Although both hypotheses predict a higher genetic diversity and lower

F_{ST} in P2, the position of P2 on the phylogenetic tree and phylogeographic history suggests the second hypothesis to be a more probable scenario. However, the two hypotheses are not mutually exclusive and might have both contributed to the genetic structure of the yellow-breasted bunting.

These identified populations partly correspond to the distribution of subspecies of yellow-breasted buntings (Copete and Sharpe 2020; Park et al. 2020). P3 falls entirely within the range of subspecies *E. a. aureola*, while P1 falls entirely within the range of *E. a. ornata* (Figure 1a). The main disagreement occurred in the East Transbaikalia, North-Eastern China, Anadyr land, and Kamchatka. Based on the genetic structure and phylogeographic history, the population in Anadyr land and Kamchatka (P3.a, highlighted in black in Figure 1b) should belong to P3, and birds in this region likely spread from East Mongolia of P3. The population in East Transbaikalia also belongs to P3. On the other hand, birds in the North-Eastern China area should belong to P2.

4.2 | The Impacts of Climate Change and Human Activities on Ancient and Recent Demographic History

Most populations of this species showed a similar pattern over the past thousands to millions of years. Notable differences in demographic history appear to occur at or after the LGM, when the populations began to diverge. The demographic patterns and effective population size of PSMC results of populations P1 and P3 were generally consistent with the previous genomics study on yellow-breasted bunting (Wang et al. 2022), which did not identify the demographic history pattern of P2. For the relatively recent demographic history, we have identified two bottlenecks in populations P2 and P3 during the LGP using SMC++, while Wang et al.'s (2022) study failed to reconstruct the demographic trajectories during this period. This may be due to the Stairwayplot having a lower resolution in recent history when the sample size was small (Liu and Fu 2015). Furthermore, our results suggest that the ancient demographic history of yellow-breasted bunting was mainly affected by global climate change. Specifically, the population of yellow-breasted bunting experienced significant declines during the LGP while showing a notable population expansion during the warmer MH period. Additionally, the changes in the suitable breeding range of yellow-breasted bunting were also in line with the population fluctuations, with the minimum distribution range occurring during the LGM. This implies that the shrinking habitat forces the populations to contract towards glacial refuges during the LGM. The combination of harsh environments and fragmented habitats resulted in population declines during the LGM (Hewitt 2004; Nadachowska-Brzyska et al. 2015). Our study aligns with previous research on 38 avian species, suggesting that many bird species experienced population contractions and expansions during the Quaternary period, coinciding with climate cycles (Nadachowska-Brzyska et al. 2015).

However, population fluctuations during the glacial period can vary among populations, even within the same species. For instance, unlike P2 and P3, P1 remained at a low level of effective population size after LGM (Figure 3d). Subsequently, P1.b recovered during the MH, while P1.a did not. This difference may be related to the geographic location of the populations. P1.a primarily inhabits islands, which are more susceptible to the effects of climate change. The cooler and drier climate during the LGM could lead to changes in vegetation zones and the fragmentation and contraction of island species' habitats (Collins et al. 2013; Tsukada 1983). Additionally, the drought may have led to a decline in food resources (such as seeds and insects) for the species, potentially contributing to a decrease in populations (Albright et al. 2010; Tsukada 1983).

Human activities have likely influenced the recent demographic history of the yellow-breasted bunting, as well as other endangered avian species (Dierickx et al. 2020). Over the past 10,000 years, we were in the stable and warm Holocene interglacial period. However, the populations of yellow-breasted bunting have undergone varying demographic trajectories. During the past 700 generations, P2 remained large and stable, while both P1 and P3 encountered two bottlenecks. The first bottleneck, which occurred 400–500 generations ago, primarily affected the restricted coastal population P1.b, leading to a drastic 100-fold decline in population size. The second bottleneck, around 100 generations ago (approximately 300 years ago), had a broader impact, resulting in a 10-fold population decline for both P1 and P3. We speculate that the recent decline in the population of yellow-breasted bunting may be attributed to human activities, such as the Second Agricultural Revolution in Europe, spanning from the mid-17th to late 19th centuries (Mingay 1977). This revolution accelerated land development and standardisation, along with the widespread use of fertilisers (Mingay 1977; Thompson 1968). Previous research suggests that agricultural intensification, especially increased use of pesticides and chemical fertilisers, likely reduced food availability for many farmland bird species by diminishing insect and invertebrate populations, particularly during breeding seasons (Donald et al. 2001; Rigal et al. 2023). Consequently, the agricultural intensification in Europe and other regions may have impacted the population size of the yellow-breasted bunting in its breeding area over the past 100 generations. Furthermore, subsequent human trapping during migration has exacerbated the decline in the population of this species (Kamp et al. 2015).

4.3 | The Impact of Demographic History on Genetic Diversity, Inbreeding, and Mutation Load

The genetic diversity of yellow-breasted buntings was strongly associated with their demographic history. Populations P1 and P3, which have undergone two recent bottlenecks, exhibit significantly lower levels of genetic diversity compared to P2. In particular, population P1.a, which has remained a smaller effective population size since LGM, shows the lowest genetic diversity. Additionally, the demographic history has also influenced the level of inbreeding in this species. Two bottlenecks over the past 700 generations have likely resulted in higher inbreeding in P1 compared to other populations. Moreover, the smaller effective population size has probably led to a higher level of inbreeding in population P1.b than in population P3, even though they have similar demographic trajectories. The demographic history of populations also had a significant impact on the accumulation of deleterious mutations. While these populations

have similar total deleterious mutations, populations P1.a and P1.b have significantly more homozygous deleterious mutations compared to the other two populations. The relatively small effective population size and high inbreeding levels in populations P1.a and P1.b may contribute to the accumulation of homozygous deleterious mutations.

Simulations further support the idea that populations having lower effective population sizes accumulate relatively more homozygous deleterious mutations. Furthermore, we found that differences in homozygous deleterious mutations among populations in the simulations were more pronounced than those in the empirical data. This may be due to gene flow between populations in real scenarios or the difference in the distribution of fitness effects we estimated for this species, which may affect the accumulation of deleterious mutations in different populations (Couvet 2002; Eyre-Walker and Keightley 2007). However, unlike other endangered species that have gone through long periods of small population sizes (Grossen et al. 2020; Kardos et al. 2023), the three yellow-breasted bunting populations still have relatively large effective population sizes, suggesting stronger purifying selection overall, like the passenger pigeon (Murray et al. 2017). However, P1.a has accumulated more LoF mutations compared to the other populations, and it has a significantly higher ratio of LoF mutations than P2. It may be attributed to P1.a still having a large population size ($N_e > 10{,}000$), as LoF mutations are generally more easily eliminated by selection in small populations. Alternatively, it is possible that P1.a did not have enough time to purge these mutations. In contrast, population P2 has a significantly lower ratio of deleterious mutations compared to the other populations, possibly due to the larger effective population size, resulting in stronger purifying selection in this population. This is in line with previous studies suggesting that the ratio of deleterious mutations is negatively correlated to effective population sizes, implying stronger purifying selection in larger populations (Bertorelle et al. 2022; Robinson et al. 2022). The higher frequency of tolerated mutations in population P2 may be influenced by recent population expansion and/or frequent gene flow between P2 and other populations. This is because the calculation of R_{xy} is based on the relative frequency of derived alleles between populations, and both population expansion and gene flow can affect the allele frequency of deleterious mutations within a population, thereby affecting the R_{xy} value of tolerated mutations (Chen et al. 2019; Do et al. 2015; Lohmueller et al. 2008).

Although the yellow-breasted bunting experienced population fluctuations similar to those of the passenger pigeons during the LGP, it did not undergo regular fluctuations as the passenger pigeons did before the LGP (Hung et al. 2014). In addition, PSMC results show that the historical N_e of yellow-breasted bunting ranged from 10^5 to 2×10^6, which is much larger than that of passenger pigeons (ranging from 4×10^4 to 2×10^5). Meanwhile, the yellow-breasted bunting exhibited a genome-wide nucleotide diversity (5.67×10^{-3}) that is twice that of the passenger pigeon ($\pi = 2.7\times10^{-3}$) (Hung et al. 2014). Moreover, the yellow-breasted bunting's genome-wide heterozygosity (4.88×10^{-3}) is much higher than the heterozygosity of the other eight endangered bird species (Table S9, ranging from 0.43×10^{-3} to 1.88×10^{-3}), although there may be some technological bias when comparing different studies (Cavill et al. 2024; Chen et al. 2023; Dussex et al. 2021; Li et al. 2014, 2022; Zhan et al. 2013). However, the yellow-breasted bunting remains at risk of extinction, particularly in light of recent population collapse. The case of the passenger pigeons serves as a stark reminder that even species with larger populations and the capacity to purge harmful mutations can still face extinction when confronted with significant environmental changes (Murray et al. 2017). Furthermore, larger populations generally contain more deleterious mutations, rendering the species more prone to inbreeding depression during substantial population declines (Bertorelle et al. 2022). Moreover, since our samples were collected from 1992 to 2004, the beginning of the recent population collapse (1980 to present), continuous population decline in recent years likely exacerbated the genetic threats in the current population, leading to an overestimation of this species' genetic health based on these samples. Indeed, when we compared the average heterozygosity estimated in the current study (4.88×10^{-3}; based on samples collected from 1992 to 2004) with that from an earlier study based on a small number of samples collected in 2019 (4.6×10^{-3}; Wang et al. 2022), the more recent samples had an average heterozygosity lower than that of P1.a and much lower than that of the other populations. This suggests a possible genetic diversity decline in the yellow-breasted bunting within the last 30 years.

4.4 | Conservation Implications

Our findings indicate the necessity to prevent the loss of genetic diversity and the increase of inbreeding in the yellow-breasted bunting. While the population before the recent population collapse exhibited relatively low genetic threats with high genetic diversity and low levels of inbreeding, the genetic threats faced by the current population remain unclear. It is essential to take measures to halt the ongoing decline of the census population size and to conduct regular quantitative and genetic monitoring. The yellow-breasted bunting population is primarily threatened by illegal hunting along migratory routes. Although China has prohibited the trade of this species since 1997 and has made improvements in law enforcement and awareness campaigns in recent years (Heim et al. 2021; Kamp et al. 2015), more attention is still required to address this issue. The other significant threat is the impact of climate change and habitat loss. Our results suggest that although climate change will not significantly affect the wintering area by 2070, it will lead to a significant reduction in the breeding area. The breeding area in the eastern distribution range will largely disappear, and the future breeding area will contract to North-Eastern Europe and Western Siberia. Farmland birds in Europe are facing ongoing population declines due to agricultural intensification (Donald et al. 2001; Rigal et al. 2023). Additionally, migratory birds such as the yellow-breasted bunting may be more vulnerable to climate change due to their limited potential for range shifts in comparison to resident birds, since they exhibit higher fidelity to breeding and wintering areas (Välimäki et al. 2016). Therefore, it is crucial to safeguard the habitat and food resources within the breeding range of the yellow-breasted bunting to mitigate the impact of climate and environmental changes.

In light of the genetic structure findings, we propose conserving the yellow-breasted bunting as one conservation unit, given the shallow genetic differentiation among the three populations and

the gene flow between them. However, additional conservation efforts are necessary for the P1 population, which consistently exhibits a lower effective population size and genetic diversity, along with more homozygous deleterious mutations. If these exposed deleterious mutations are not promptly purged, they could impact the population's overall fitness (Hedrick and Garcia-Dorado 2016). Specifically, the island population, P1.a, is particularly vulnerable to climate change and other stochastic factors due to the isolated location and worse genetic health. To prevent the localised extinction of this population, as seen in Finland (Copete and Sharpe 2020), long-term population and genetic monitoring, as well as habitat protection, should be implemented. The case of P1.a demonstrates that even populations with a large effective population size are susceptible to genetic threats—such as increased inbreeding and accumulations of homozygous deleterious mutations (realised load)—during rapid population declines. These findings have broad implications for conservation management of endangered species with relatively large populations.

Author Contributions

Conceptualization: S.Y.W.S.; sample collection: S.Y.W.S. and G.C.; methodology and lab works: G.C. and S.Y.W.S.; analysis: G.C.; visualisation: G.C.; writing – original draft: G.C.; writing – review and editing: all authors; supervision, project administration, and funding acquisition: S.Y.W.S.

Acknowledgements

We thank the University of Washington Burke Museum and the University of Minnesota Bell Museum for providing specimen loans. This project was supported by the General Research Fund (from the Research Grant Council, University Grants Committee, Hong Kong) granted to S.Y.W.S. (project number: 17124422). We also thank the computing resources provided by the Information Technology Services at the University of Hong Kong. We also thank Dr. Alison Cloutier for her valuable comments.

Disclosure

Benefit-Sharing Statement: Benefits Generated: The samples used in this study were obtained from museum collections, as we mentioned in Section 2 and "Acknowledgments" sections. Our research provides essential genetic information for a critically endangered species, which will significantly aid future conservation efforts. Additionally, all data generated from this study is shared with the public through open-access databases.

Conflicts of Interest

The authors declare no conflicts of interest.

Data Availability Statement

The *Emberiza aureola* reference genome used in this study is available at the National Center for Biotechnology Information (NCBI) with accession number JBNGPE000000000 (BioSample SAMN47298012, BioProject PRJNA1234483). The genetic data and code used in this study are available at https://zenodo.org/records/15515775.

References

Albright, T. P., A. M. Pidgeon, C. D. Rittenhouse, et al. 2010. "Effects of Drought on Avian Community Structure." *Global Change Biology* 16, no. 8: 2158–2170. https://doi.org/10.1111/j.1365-2486.2009.02120.x.

Alexander, D. H., J. Novembre, and K. Lange. 2009. "Fast Model-Based Estimation of Ancestry in Unrelated Individuals." *Genome Research* 19, no. 9: 1655–1664. https://doi.org/10.1101/gr.094052.109.

Andrews, S. 2010. "FastQC: A Quality Control Tool for High Throughput Sequence Data." https://www.bioinformatics.babraham.ac.uk/projects/fastqc/.

Backstrom, N., W. Forstmeier, H. Schielzeth, et al. 2010. "The Recombination Landscape of the Zebra Finch *Taeniopygia guttata* Genome." *Genome Research* 20, no. 4: 485–495. https://doi.org/10.1101/gr.101410.109.

Bertorelle, G., F. Raffini, M. Bosse, et al. 2022. "Genetic Load: Genomic Estimates and Applications in Non-Model Animals." *Nature Reviews Genetics* 23, no. 8: 492–503. https://doi.org/10.1038/s41576-022-00448-x.

BirdLife International. 2024. "Species Factsheet: *Emberiza aureola*." https://datazone.birdlife.org/species/factsheet/yellow-breasted-bunting-emberiza-aureola. (Accessed on 07/05/2024).

Blomqvist, D., A. Pauliny, M. Larsson, and L. Å. Flodin. 2010. "Trapped in the Extinction Vortex? Strong Genetic Effects in a Declining Vertebrate Population." *BMC Evolutionary Biology* 10: 1–9. https://doi.org/10.1186/1471-2148-10-33.

Bouckaert, R., J. Heled, D. Kühnert, et al. 2014. "BEAST 2: A Software Platform for Bayesian Evolutionary Analysis." *PLoS Computational Biology* 10, no. 4: e1003537. https://doi.org/10.1371/journal.pcbi.1003537.

Broad Institute. 2019. "Picard Toolkit." http://broadinstitute.github.io/picard/.

Cavill, E. L., H. E. Morales, X. Sun, et al. 2024. "When Birds of a Feather Flock Together: Severe Genomic Erosion and the Implications for Genetic Rescue in an Endangered Island Passerine." *Evolutionary Applications* 17, no. 7: e13739. https://doi.org/10.1111/eva.13739.

Ceballos, F. C., P. K. Joshi, D. W. Clark, M. Ramsay, and J. F. Wilson. 2018. "Runs of Homozygosity: Windows Into Population History and Trait Architecture." *Nature Reviews Genetics* 19, no. 4: 220–234. https://doi.org/10.1038/nrg.2017.109.

Chen, G., C. Zheng, L. Peng, et al. 2023. "Long-Term and Extensive Population Decline Drives Elevated Expression of Genetic Load in a Critically Endangered Seabird." *Research Square*. https://doi.org/10.21203/rs.3.rs-2960319/v1.

Chen, N., I. Juric, E. J. Cosgrove, et al. 2019. "Allele Frequency Dynamics in a Pedigreed Natural Population." *Proceedings of the National Academy of Sciences of the United States of America* 116, no. 6: 2158–2164. https://doi.org/10.1073/pnas.1813852116.

Chen, S. F., Y. Q. Zhou, Y. R. Chen, and J. Gu. 2018. "Fastp: An Ultra-Fast All-In-One FASTQ Preprocessor." *Bioinformatics* 34, no. 17: 884–890. https://doi.org/10.1093/bioinformatics/bty560.

Chevreux, B., T. Pfisterer, B. Drescher, et al. 2004. "Using the miraEST Assembler for Reliable and Automated mRNA Transcript Assembly and SNP Detection in Sequenced ESTs." *Genome Research* 14, no. 6: 1147–1159. https://doi.org/10.1101/gr.1917404.

Cingolani, P., A. Platts, L. L. Wang, et al. 2012. "A Program for Annotating and Predicting the Effects of Single Nucleotide Polymorphisms, SnpEff: SNPs in the Genome of *Drosophila melanogaster* Strain w1118; Iso-2; Iso-3." *Fly* 6, no. 2: 80–92. https://doi.org/10.4161/fly.19695.

Collins, A. F., M. B. Bush, and J. P. Sachs. 2013. "Microrefugia and Species Persistence in the Galápagos Highlands: A 26,000-Year Paleoecological Perspective." *Frontiers in Genetics* 4: 269. https://doi.org/10.3389/fgene.2013.00269.

Copete, J. L., and C. J. Sharpe. 2020. "Yellow-Breasted Bunting (*Emberiza aureola*), Version 1.0." In *Birds of the World*, edited by J. del Hoyo, A. Elliott, J. Sargatal, D. A. Christie, and E. de Juana. Cornell Lab of Ornithology. https://doi.org/10.2173/bow.yebbun.01.

Couvet, D. 2002. "Deleterious Effects of Restricted Gene Flow in Fragmented Populations." *Conservation Biology* 16, no. 2: 369–376. https://doi.org/10.1046/j.1523-1739.2002.99518.x.

Cowie, R. H., P. Bouchet, and B. Fontaine. 2022. "The Sixth Mass Extinction: Fact, Fiction or Speculation?" *Biological Reviews* 97, no. 2: 640–663. https://doi.org/10.1111/brv.12816.

Danecek, P., A. Auton, G. Abecasis, et al. 2011. "The Variant Call Format and VCFtools." *Bioinformatics* 27, no. 15: 2156–2158. https://doi.org/10.1093/bioinformatics/btr330.

De Laet, J., and J. D. Summers-Smith. 2007. "The Status of the Urban House Sparrow in North-Western Europe: A Review." *Journal of Ornithology* 148: S275–S278. https://doi.org/10.1007/s10336-007-0154-0.

Dierickx, E. G., S. Y. W. Sin, H. P. J. van Veelen, et al. 2020. "Genetic Diversity, Demographic History and Neo-Sex Chromosomes in the Critically Endangered Raso Lark." *Proceedings of the Royal Society B: Biological Sciences* 287, no. 1922: 20192613. https://doi.org/10.1098/rspb.2019.2613.

Dixon, P. 2003. "VEGAN, a Package of R Functions for Community Ecology." *Journal of Vegetation Science* 14, no. 6: 927–930. https://doi.org/10.1111/j.1654-1103.2003.tb02228.x.

Do, R., D. Balick, H. Li, I. Adzhubei, S. Sunyaev, and D. Reich. 2015. "No Evidence That Selection has Been Less Effective at Removing Deleterious Mutations in Europeans Than in Africans." *Nature Genetics* 47, no. 2: 126–131. https://doi.org/10.1038/ng.3186.

Donald, P. F., R. E. Green, and M. F. Heath. 2001. "Agricultural Intensification and the Collapse of Europe's Farmland Bird Populations." *Proceedings of the Royal Society of London, Series B: Biological Sciences* 268, no. 1462: 25–29. https://doi.org/10.1098/rspb.2000.1325.

Dussex, N., T. Van Der Valk, H. E. Morales, et al. 2021. "Population Genomics of the Critically Endangered Kākāpō." *Cell Genomics* 1, no. 1: 100002. https://doi.org/10.1016/j.xgen.2021.100002.

Edwards, C. J., M. A. Suchard, P. Lemey, et al. 2011. "Ancient Hybridization and an Irish Origin for the Modern Polar Bear Matriline." *Current Biology* 21, no. 15: 1251–1258. https://doi.org/10.1016/j.cub.2011.05.058.

Eyre-Walker, A., and P. D. Keightley. 2007. "The Distribution of Fitness Effects of New Mutations." *Nature Reviews Genetics* 8, no. 8: 610–618. https://doi.org/10.1038/nrg2146.

Fagan, W. F., and E. E. Holmes. 2006. "Quantifying the Extinction Vortex." *Ecology Letters* 9, no. 1: 51–60. https://doi.org/10.1111/j.1461-0248.2005.00845.x.

Fitak, R. R. 2021. "OptM: Estimating the Optimal Number of Migration Edges on Population Trees Using Treemix." *Biology Methods & Protocols* 6, no. 1: bpab017. https://doi.org/10.1093/biomethods/bpab017.

Flynn, J. M., R. Hubley, C. Goubert, et al. 2020. "RepeatModeler2 for Automated Genomic Discovery of Transposable Element Families." *Proceedings of the National Academy of Sciences of the United States of America* 117, no. 17: 9451–9457. https://doi.org/10.1073/pnas.1921046117.

Frankham, R., J. D. Ballou, and D. A. Briscoe. 2010. *Introduction to Conservation Genetics*. 2nd ed. Cambridge University Press.

Gandra, M., J. Assis, M. R. Martins, and D. Abecasis. 2021. "Reduced Global Genetic Differentiation of Exploited Marine Fish Species." *Molecular Biology and Evolution* 38, no. 4: 1402–1412. https://doi.org/10.1093/molbev/msaa299.

Glemin, S. 2003. "How Are Deleterious Mutations Purged? Drift Versus Nonrandom Mating." *Evolution* 57, no. 12: 2678–2687. https://doi.org/10.1111/j.0014-3820.2003.tb01512.x.

Grabherr, M. G., P. Russell, M. Meyer, et al. 2010. "Genome-Wide Synteny Through Highly Sensitive Sequence Alignment: Satsuma." *Bioinformatics* 26, no. 9: 1145–1151. https://doi.org/10.1093/bioinformatics/btq102.

Grantham, R. 1974. "Amino-Acid Difference Formula to Help Explain Protein Evolution." *Science* 185, no. 4154: 862–864. https://doi.org/10.1126/science.185.4154.862.

Grossen, C., F. Guillaume, L. F. Keller, and D. Croll. 2020. "Purging of Highly Deleterious Mutations Through Severe Bottlenecks in Alpine Ibex." *Nature Communications* 11, no. 1: 1001. https://doi.org/10.1038/s41467-020-14803-1.

Hahn, C., L. Bachmann, and B. Chevreux. 2013. "Reconstructing Mitochondrial Genomes Directly From Genomic Next-Generation Sequencing Reads—A Baiting and Iterative Mapping Approach." *Nucleic Acids Research* 41, no. 13: e129. https://doi.org/10.1093/nar/gkt371.

Haller, B. C., and P. W. Messer. 2023. "SLiM 4: Multispecies Eco-Evolutionary Modeling." *American Naturalist* 201, no. 5: 127–139. https://doi.org/10.1086/723601.

Hannon, G. J. 2010. "Fastx-Toolkit." http://hannonlab.cshl.edu/fastx_toolkit/.

Hedrick, P. W., and A. Garcia-Dorado. 2016. "Understanding Inbreeding Depression, Purging, and Genetic Rescue." *Trends in Ecology & Evolution* 31, no. 12: 940–952. https://doi.org/10.1016/j.tree.2016.09.005.

Heim, W., S. Chan, N. Hölzel, P. Ktitorov, A. Mischenko, and J. Kamp. 2021. "East Asian Buntings: Ongoing Illegal Trade and Encouraging Conservation Responses." *Conservation Science and Practice* 3, no. 6: e405. https://doi.org/10.1111/csp2.405.

Hewitt, G. M. 2004. "Genetic Consequences of Climatic Oscillations in the Quaternary." *Philosophical Transactions of the Royal Society, B: Biological Sciences* 359, no. 1442: 183–195. https://doi.org/10.1098/rstb.2003.1388.

Hijmans, R. J., E. Williams, C. Vennes, and M. R. J. Hijmans. 2017. "Package 'Geosphere'." *Spherical Trigonometry* 1, no. 7: 1–45.

Holm, S. R., and J. C. Svenning. 2014. "180,000 Years of Climate Change in Europe: Avifaunal Responses and Vegetation Implications." *PLoS One* 9, no. 4: e94021. https://doi.org/10.1371/journal.pone.0094021.

Holt, C., and M. Yandell. 2011. "MAKER2: An Annotation Pipeline and Genome-Database Management Tool for Second-Generation Genome Projects." *BMC Bioinformatics* 12: 1–14. https://doi.org/10.1186/1471-2105-12-491.

Hung, C. M., P. J. L. Shaner, R. M. Zink, et al. 2014. "Drastic Population Fluctuations Explain the Rapid Extinction of the Passenger Pigeon." *Proceedings of the National Academy of Sciences of the United States of America* 111, no. 29: 10636–10641. https://doi.org/10.1073/pnas.1401526111.

Huynh, S., A. Cloutier, G. L. Chen, et al. 2023. "Whole-Genome Analyses Reveal Past Population Fluctuations and Low Genetic Diversities of the North Pacific Albatrosses." *Molecular Biology and Evolution* 40, no. 7: msad155. https://doi.org/10.1093/molbev/msad155.

Inger, R., R. Gregory, J. P. Duffy, I. Stott, P. Vorisek, and K. J. Gaston. 2015. "Common European Birds Are Declining Rapidly While Less Abundant Species' Numbers Are Rising." *Ecology Letters* 18, no. 1: 28–36. https://doi.org/10.1111/ele.12387.

Jombart, T. 2008. "Adegenet: A R Package for the Multivariate Analysis of Genetic Markers." *Bioinformatics* 24, no. 11: 1403–1405. https://doi.org/10.1093/bioinformatics/btn129.

Jombart, T., and I. Ahmed. 2011. "Adegenet 1.3-1: New Tools for the Analysis of Genome-Wide SNP Data." *Bioinformatics* 27, no. 21: 3070–3071. https://doi.org/10.1093/bioinformatics/btr521.

Kalinowski, S. T. 2011. "The Computer Program STRUCTURE Does Not Reliably Identify the Main Genetic Clusters Within Species: Simulations and Implications for Human Population Structure." *Heredity* 106, no. 4: 625–632. https://doi.org/10.1038/hdy.2010.95.

Kamp, J., S. Oppel, A. A. Ananin, et al. 2015. "Global Population Collapse in a Superabundant Migratory Bird and Illegal Trapping in

China." *Conservation Biology* 29, no. 6: 1684–1694. https://doi.org/10.1111/cobi.12537.

Kardos, M., E. E. Armstrong, S. W. Fitzpatrick, et al. 2021. "The Crucial Role of Genome-Wide Genetic Variation in Conservation." *Proceedings of the National Academy of Sciences of the United States of America* 118, no. 48: e2104642118. https://doi.org/10.1073/pnas.2104642118.

Kardos, M., H. R. Taylor, H. Ellegren, G. Luikart, and F. W. Allendorf. 2016. "Genomics Advances the Study of Inbreeding Depression in the Wild." *Evolutionary Applications* 9, no. 10: 1205–1218. https://doi.org/10.1111/eva.12414.

Kardos, M., Y. L. Zhang, K. M. Parsons, et al. 2023. "Inbreeding Depression Explains Killer Whale Population Dynamics." *Nature Ecology & Evolution* 7, no. 5: 675–686. https://doi.org/10.1038/s41559-023-01995-0.

Keilwagen, J., F. Hartung, and J. Grau. 2019. "GeMoMa: Homology-Based Gene Prediction Utilizing Intron Position Conservation and RNA-Seq Data." *Methods in Molecular Biology* 1962: 161–177. https://doi.org/10.1007/978-1-4939-9173-0_9.

Keller, L. F., and D. M. Waller. 2002. "Inbreeding Effects in Wild Populations." *Trends in Ecology & Evolution* 17, no. 5: 230–241. https://doi.org/10.1016/S0169-5347(02)02489-8.

Kim, B. Y., C. D. Huber, and K. E. Lohmueller. 2017. "Inference of the Distribution of Selection Coefficients for New Nonsynonymous Mutations Using Large Samples." *Genetics* 206, no. 1: 345–361. https://doi.org/10.1534/genetics.116.197145.

Kyriazis, C. C., A. C. Beichman, K. E. Brzeski, et al. 2023. "Genomic Underpinnings of Population Persistence in Isle Royale Moose." *Molecular Biology and Evolution* 40, no. 2: msad021. https://doi.org/10.1093/molbev/msad021.

Kyriazis, C. C., R. K. Wayne, and K. E. Lohmueller. 2021. "Strongly Deleterious Mutations Are a Primary Determinant of Extinction Risk due to Inbreeding Depression." *Evolution Letters* 5, no. 1: 33–47. https://doi.org/10.1002/evl3.209.

Lam, D. K., A. C. Frantz, T. Burke, E. Geffen, and S. Y. W. Sin. 2023. "Both Selection and Drift Drive the Spatial Pattern of Adaptive Genetic Variation in a Wild Mammal." *Evolution* 77, no. 1: 221–238. https://doi.org/10.1093/evolut/qpac014.

Lemey, P., A. Rambaut, A. J. Drummond, and M. A. Suchard. 2009. "Bayesian Phylogeography Finds Its Roots." *PLoS Computational Biology* 5, no. 9: e1000520. https://doi.org/10.1371/journal.pcbi.1000520.

Li, H., and R. Durbin. 2009. "Fast and Accurate Short Read Alignment With Burrows-Wheeler Transform." *Bioinformatics* 25, no. 14: 1754–1760. https://doi.org/10.1093/bioinformatics/btp324.

Li, H., and R. Durbin. 2011. "Inference of Human Population History From Individual Whole-Genome Sequences." *Nature* 475, no. 7357: 493–496. https://doi.org/10.1038/nature10231.

Li, H., B. Handsaker, A. Wysoker, et al. 2009. "The Sequence Alignment/Map Format and SAMtools." *Bioinformatics* 25, no. 16: 2078–2079. https://doi.org/10.1093/bioinformatics/btp352.

Li, S. B., B. Li, C. Cheng, et al. 2014. "Genomic Signatures of Near-Extinction and Rebirth of the Crested Ibis and Other Endangered Bird Species." *Genome Biology* 15, no. 12: 1–17. https://doi.org/10.1186/S13059-014-0557-1.

Li, S. H., Y. Liu, C. F. Yeh, et al. 2022. "Not out of the Woods Yet: Signatures of the Prolonged Negative Genetic Consequences of a Population Bottleneck in a Rapidly Re-Expanding Wader, the Black-Faced Spoonbill *Platalea minor*." *Molecular Ecology* 31, no. 2: 529–545. https://doi.org/10.1111/mec.16260.

Liu, X. M., and Y. X. Fu. 2015. "Exploring Population Size Changes Using SNP Frequency Spectra." *Nature Genetics* 47, no. 5: 555–559. https://doi.org/10.1038/ng.3254.

Liu, Y. C., J. Schröder, and B. Schmidt. 2013. "Musket: A Multistage k-Mer Spectrum Based Error Corrector for Illumina Sequence Data." *Bioinformatics* 29, no. 3: 308–315. https://doi.org/10.1093/bioinformatics/bts690.

Lohmueller, K. E., A. R. Indap, S. Schmidt, et al. 2008. "Proportionally More Deleterious Genetic Variation in European Than in African Populations." *Nature* 451, no. 7181: 994–U995. https://doi.org/10.1038/nature06611.

Malinsky, M., M. Matschiner, and H. Svardal. 2021. "Dsuite – Fast D-Statistics and Related Admixture Evidence From VCF Files." *Molecular Ecology Resources* 21, no. 2: 584–595. https://doi.org/10.1111/1755-0998.13265.

Manichaikul, A., J. C. Mychaleckyj, S. S. Rich, K. Daly, M. Sale, and W. M. Chen. 2010. "Robust Relationship Inference in Genome-Wide Association Studies." *Bioinformatics* 26, no. 22: 2867–2873. https://doi.org/10.1093/bioinformatics/btq559.

McKenna, A., M. Hanna, E. Banks, et al. 2010. "The Genome Analysis Toolkit: A MapReduce Framework for Analyzing Next-Generation DNA Sequencing Data." *Genome Research* 20, no. 9: 1297–1303. https://doi.org/10.1101/gr.107524.110.

Mingay, G. E. 1977. *The Agricultural Revolution: Changes in Agriculture, 1650–1880*. London: Adam & Charles Black.

Minh, B. Q., H. A. Schmidt, O. Chernomor, et al. 2020. "IQ-TREE 2: New Models and Efficient Methods for Phylogenetic Inference in the Genomic Era." *Molecular Biology and Evolution* 37, no. 5: 1530–1534. https://doi.org/10.1093/molbev/msaa015.

Murray, G. G. R., A. E. R. Soares, B. J. Novak, et al. 2017. "Natural Selection Shaped the Rise and Fall of Passenger Pigeon Genomic Diversity." *Science* 358, no. 6365: 951–954. https://doi.org/10.1126/science.aao0960.

Nadachowska-Brzyska, K., C. Li, L. Smeds, G. J. Zhang, and H. Ellegren. 2015. "Temporal Dynamics of Avian Populations During Pleistocene Revealed by Whole-Genome Sequences." *Current Biology* 25, no. 10: 1375–1380. https://doi.org/10.1016/j.cub.2015.03.047.

Pan, T., L. Ren, X. Zhu, et al. 2015. "Mitochondrial Genome of the *Emberiza aureola* (Emberizidae: *Emberiza*)." *Mitochondrial DNA* 26, no. 1: 121–122. https://doi.org/10.3109/19401736.2013.814112.

Park, J.-G., C.-U. Park, K.-S. Jin, et al. 2020. "Moult and Plumage Patterns of the Critically Endangered Yellow-Breasted Bunting (*Emberiza aureola*) at a Stopover Site in Korea." *Journal of Ornithology* 161, no. 1: 257–266. https://doi.org/10.1007/s10336-019-01716-0.

Patterson, N., P. Moorjani, Y. T. Luo, et al. 2012. "Ancient Admixture in Human History." *Genetics* 192, no. 3: 1065–1093. https://doi.org/10.1534/genetics.112.145037.

Peter, B. M. 2016. "Admixture, Population Structure, and F-Statistics." *Genetics* 202, no. 4: 1485–1501. https://doi.org/10.1534/genetics.115.183913.

Phillips, S. J., R. P. Anderson, and R. E. Schapire. 2006. "Maximum Entropy Modeling of Species Geographic Distributions." *Ecological Modelling* 190, no. 3–4: 231–259. https://doi.org/10.1016/j.ecolmodel.2005.03.026.

Pickrell, J. K., and J. K. Pritchard. 2012. "Inference of Population Splits and Mixtures From Genome-Wide Allele Frequency Data." *PLoS Genetics* 8, no. 11: 1. https://doi.org/10.1371/journal.pgen.1002967.

Price, M. N., P. S. Dehal, and A. P. Arkin. 2010. "FastTree 2-Approximately Maximum-Likelihood Trees for Large Alignments." *PLoS One* 5, no. 3: e9490. https://doi.org/10.1371/journal.pone.0009490.

Purcell, S., B. Neale, K. Todd-Brown, et al. 2007. "PLINK: A Tool Set for Whole-Genome Association and Population-Based Linkage Analyses." *American Journal of Human Genetics* 81, no. 3: 559–575. https://doi.org/10.1086/519795.

Rigal, S., V. Dakos, H. Alonso, et al. 2023. "Farmland Practices Are Driving Bird Population Decline Across Europe." *Proceedings of the National Academy of Sciences of the United States of America* 120, no. 21: e2216573120. https://doi.org/10.1073/pnas.2216573120.

Robinson, J. A., C. C. Kyriazis, S. F. Nigenda-Morales, et al. 2022. "The Critically Endangered Vaquita Is Not Doomed to Extinction by Inbreeding Depression." *Science* 376, no. 6593: 635–639. https://doi.org/10.1126/science.abm1742.

Robinson, J. A., J. Raikkonen, L. M. Vucetich, et al. 2019. "Genomic Signatures of Extensive Inbreeding in Isle Royale Wolves, a Population on the Threshold of Extinction." *Science Advances* 5, no. 5: eaau0757. https://doi.org/10.1126/sciadv.aau0757.

Santiago, E., I. Novo, A. F. Pardinas, M. Saura, J. L. Wang, and A. Caballero. 2020. "Recent Demographic History Inferred by High-Resolution Analysis of Linkage Disequilibrium." *Molecular Biology and Evolution* 37, no. 12: 3642–3653. https://doi.org/10.1093/molbev/msaa169.

Schorger, A. W. 1995. *The Passenger Pigeon: Its Natural History and Extinction*. Norman: University of Oklahoma Press.

Simao, F. A., R. M. Waterhouse, P. Ioannidis, E. V. Kriventseva, and E. M. Zdobnov. 2015. "BUSCO: Assessing Genome Assembly and Annotation Completeness With Single-Copy Orthologs." *Bioinformatics* 31, no. 19: 3210–3212. https://doi.org/10.1093/bioinformatics/btv351.

Simonsen, M., T. Mailund, and C. N. Pedersen. 2008. "Rapid Neighbour-Joining." In *Algorithms in Bioinformatics: 8th International Workshop (WABI 2008)*, 113–122. Springer. https://doi.org/10.1007/978-3-540-87361-7_10.

Sin, S. Y. W., B. A. Hoover, G. A. Nevitt, and S. V. Edwards. 2021. "Demographic History, Not Mating System, Explains Signatures of Inbreeding and Inbreeding Depression in a Large Outbred Population." *American Naturalist* 197, no. 6: 658–676. https://doi.org/10.1086/714079.

Smeds, L., A. Qvarnström, and H. Ellegren. 2016. "Direct Estimate of the Rate of Germline Mutation in a Bird." *Genome Research* 26, no. 9: 1211–1218. https://doi.org/10.1101/gr.204669.116.

Smit, A. F. A., R. Hubley, and P. Green. 2020. "RepeatMasker." *Biotech Software & Internet Report* 1, no. 1–2: 36-39. http://www.repeatmasker.org.

Smith, H. G., A. Ryegård, and S. Svensson. 2012. "Is the Large-Scale Decline of the Starling Related to Local Changes in Demography?" *Ecography* 35, no. 8: 741–748. https://doi.org/10.1111/j.1600-0587.2011.06310.x.

Snyder, C. W. 2016. "Evolution of Global Temperature Over the Past Two Million Years." *Nature* 538, no. 7624: 226–228. https://doi.org/10.1038/nature19798.

Suchard, M. A., R. E. Weiss, and J. S. Sinsheimer. 2001. "Bayesian Selection of Continuous-Time Markov Chain Evolutionary Models." *Molecular Biology and Evolution* 18, no. 6: 1001–1013. https://doi.org/10.1093/oxfordjournals.molbev.a003872.

Tamada, K., S. Hayama, M. Umeki, M. Takada, and M. Tomizawa. 2017. "Drastic Declines in Brown Shrike and Yellow-Breasted Bunting at the Lake Utonai Bird Sanctuary, Hokkaido." *Ornithological Science* 16, no. 1: 51–57. https://doi.org/10.2326/osj.16.51.

Tamada, K., M. Tomizawa, M. Umeki, and M. Takada. 2014. "Population Trends of Grassland Birds in Hokkaido, Focussing on the Drastic Decline of the Yellow-Breasted Bunting." *Ornithological Science* 13, no. 1: 29–40. https://doi.org/10.2326/osj.13.29.

Tataru, P., and T. Bataillon. 2019. "polyDFEv2.0: Testing for Invariance of the Distribution of Fitness Effects Within and Across Species." *Bioinformatics* 35, no. 16: 2868–2869. https://doi.org/10.1093/bioinformatics/bty1060.

Terhorst, J., J. A. Kamm, and Y. S. Song. 2017. "Robust and Scalable Inference of Population History From Hundreds of Unphased Whole Genomes." *Nature Genetics* 49, no. 2: 303–309. https://doi.org/10.1038/ng.3748.

Thompson, E. A. 2013. "Identity by Descent: Variation in Meiosis, Across Genomes, and in Populations." *Genetics* 194, no. 2: 301–326. https://doi.org/10.1534/genetics.112.148825.

Thompson, F. M. L. 1968. "The Second Agricultural Revolution, 1815-1880." *Economic History Review* 21, no. 1: 62–77. https://doi.org/10.2307/2592204.

Tsukada, M. 1983. "Vegetation and Climate During the Last Glacial Maximum in Japan." *Quaternary Research* 19, no. 2: 212–235. https://doi.org/10.1016/0033-5894(83)90006-6.

Välimäki, K., A. Lindén, and A. Lehikoinen. 2016. "Velocity of Density Shifts in Finnish Landbird Species Depends on Their Migration Ecology and Body Mass." *Oecologia* 181, no. 1: 313–321. https://doi.org/10.1007/s00442-015-3525-x.

van Oosterhout, C., S. A. Speak, T. Birley, et al. 2022. "Genomic Erosion in the Assessment of Species Extinction Risk and Recovery Potential." *BioRxiv* pp. 2022-2009. https://doi.org/10.1101/2022.09.13.507768.

van Vuuren, D. P., J. Edmonds, M. Kainuma, et al. 2011. "The Representative Concentration Pathways: An Overview." *Climatic Change* 109, no. 1: 5–31. https://doi.org/10.1007/s10584-011-0148-z.

Wang, I. J. 2013. "Examining the Full Effects of Landscape Heterogeneity on Spatial Genetic Variation: A Multiple Matrix Regression Approach for Quantifying Geographic and Ecological Isolation." *Evolution* 67, no. 12: 3403–3411. https://doi.org/10.1111/evo.12134.

Wang, I. J., R. E. Glor, and J. B. Losos. 2013. "Quantifying the Roles of Ecology and Geography in Spatial Genetic Divergence." *Ecology Letters* 16, no. 2: 175–182. https://doi.org/10.1111/ele.12025.

Wang, P. C., R. Hou, Y. Wu, Z. W. Zhang, P. J. Que, and P. Chen. 2022. "Genomic Status of Yellow-Breasted Bunting Following Recent Rapid Population Decline." *iScience* 25, no. 7: 104501. https://doi.org/10.1016/j.isci.2022.104501.

Xu, H. B., X. Luo, J. Qian, et al. 2012. "FastUniq: A Fast de Novo Duplicates Removal Tool for Paired Short Reads." *PLoS One* 7, no. 12: e52249. https://doi.org/10.1371/journal.pone.0052249.

Xue, Y. L., J. Prado-Martinez, P. H. Sudmant, et al. 2015. "Mountain Gorilla Genomes Reveal the Impact of Long-Term Population Decline and Inbreeding." *Science* 348, no. 6231: 242–245. https://doi.org/10.1126/science.aaa3952.

Zhan, X. J., S. K. Pan, J. Y. Wang, et al. 2013. "Peregrine and Saker Falcon Genome Sequences Provide Insights Into Evolution of a Predatory Lifestyle." *Nature Genetics* 45, no. 5: 563. https://doi.org/10.1038/ng.2588.

Zheng, G. X. Y., B. T. Lau, M. Schnall-Levin, et al. 2016. "Haplotyping Germline and Cancer Genomes With High-Throughput Linked-Read Sequencing." *Nature Biotechnology* 34, no. 3: 303–311. https://doi.org/10.1038/nbt.3432.

Zheng, Y. C., and A. Janke. 2018. "Gene Flow Analysis Method, the D-Statistic, Is Robust in a Wide Parameter Space." *BMC Bioinformatics* 19: 10. https://doi.org/10.1186/s12859-017-2002-4.

Supporting Information

Additional supporting information can be found online in the Supporting Information section.